iScience

CellPress
OPEN ACCESS

Article

TET2 is recruited by CREB to promote *Cebpb*, *Cebpa*, and *Pparg* transcription by facilitating hydroxymethylation during adipocyte differentiation

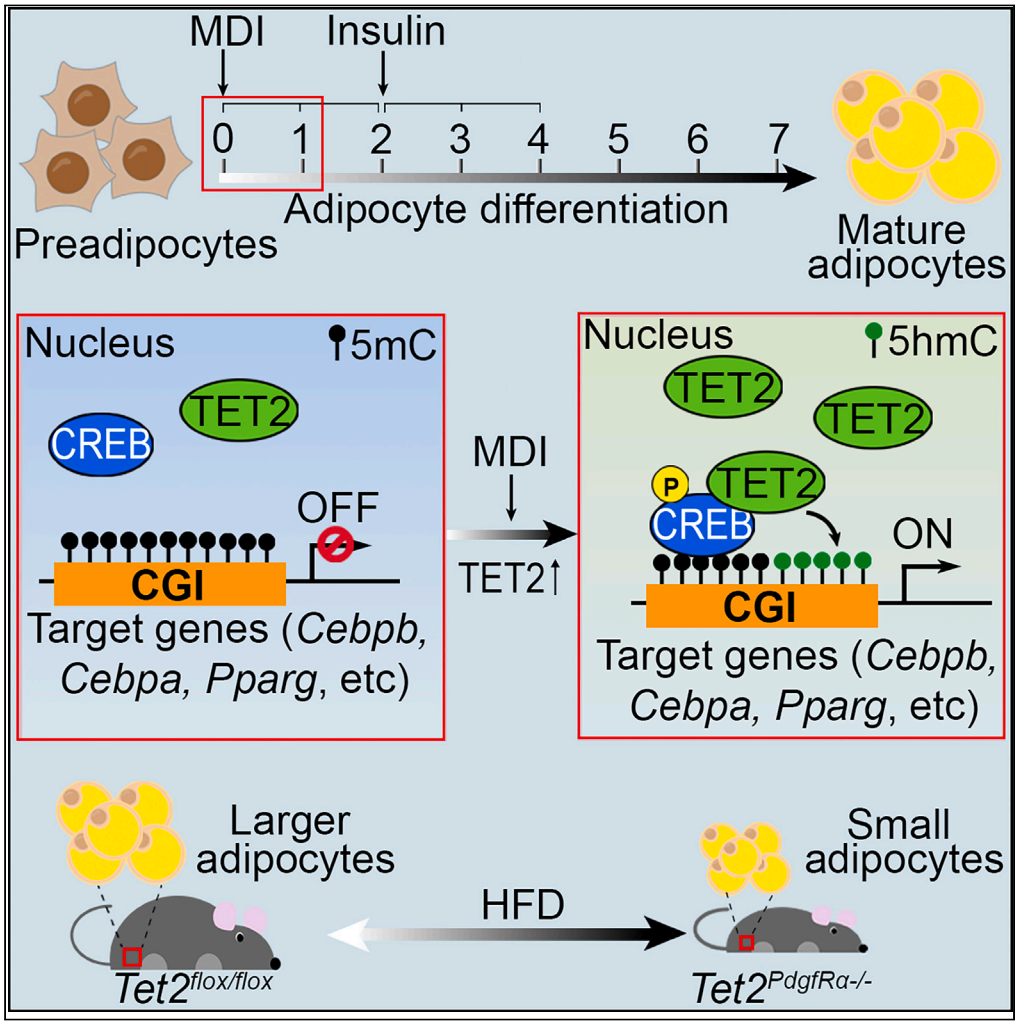

Yunjia Liu, Ting He, Zhuofang Li, ..., Huiling Guo, Rui Zhang, Boan Li

ghuiling@xmu.edu.cn (H.G.)
raissarui@foxmail.com (R.Z.)
bali@xmu.edu.cn (B.L.)

Highlights

TET2 promotes *Cebpb*, *Cebpa*, and *Pparg* expression during adipocyte differentiation

TET2 promotes 5hmC upregulation at the initial stage of adipogenic gene expression

CREB is required for TET2 enrichment and 5hmC upregulation on adipogenic genes

TET2 deficiency inhibits adipocyte enlargement and HFD-induced obesity

Liu et al., iScience *26*, 108312
November 17, 2023
https://doi.org/10.1016/j.isci.2023.108312

iScience

CellPress
OPEN ACCESS

Article

TET2 is recruited by CREB to promote *Cebpb*, *Cebpa*, and *Pparg* transcription by facilitating hydroxymethylation during adipocyte differentiation

Yunjia Liu,[1,5] Ting He,[1,5] Zhuofang Li,[1,5] Zhen Sun,[1,5] Shuai Wang,[1,3] Huanming Shen,[1] Lingfeng Hou,[1] Shengnan Li,[4] Yixin Wei,[1] Bingzhao Zhuo,[1] Shanni Li,[1] Can Zhou,[1] Huiling Guo,[1,*] Rui Zhang,[2,*] and Boan Li[1,6,*]

SUMMARY

Ten-eleven translocation proteins (TETs) are dioxygenases that convert 5-methylcytosine (5mC) to 5-hydroxymethylcytosine (5hmC), an important epigenetic mark that regulates gene expression during development and differentiation. Here, we found that the TET2 expression was positively associated with adipogenesis. Further, *in vitro* and *in vivo* experiments showed that TET2 deficiency blocked adipogenesis by inhibiting the expression of the key transcription factors CCAAT/enhancer-binding protein beta (C/EBPβ), C/EBPα and peroxisome proliferator-activated receptor gamma (PPARγ). In addition, TET2 promoted 5hmC on the CpG islands (CGIs) of *Cebpb*, *Cebpa* and *Pparg* at the initial time point of their transcription, which requires the cAMP-responsive element-binding protein (CREB). At last, specific knockout of *Tet2* in preadipocytes enabled mice to resist obesity and attenuated the obesity-associated insulin resistance. Together, TET2 is recruited by CREB to promote the expression of *Cebpb*, *Cebpa* and *Pparg* via 5hmC during adipogenesis and may be a potential therapeutic target for obesity and insulin resistance.

INTRODUCTION

5-Hydroxymethylcytosine (5hmC) is a prominent epigenetic modification established by Fe(II)- and α-ketoglutarate-dependent DNA dioxygenases belonging to the ten-eleven translocation family, including TET1, TET2, and TET3.[1] TETs catalyze the oxidation of 5-methylcytosine (5mC) to 5hmC and further to 5-formylcytosine (5fC) and 5-carboxylcytosine (5caC). 5hmC is preferentially enriched in the gene bodies, promoters and enhancers of transcriptionally active genes.[2,3] The 5hmC level in the gene body is positively correlated with gene expression in mouse embryotic stem cells (mESCs),[4] mouse brains[2] and human tissues,[3] suggesting that 5hmC may play roles in transcriptional activation.

The global content of 5hmC varies widely in different tissues, ranging from 0.06% in the spleen to nearly 0.7% in the cerebral cortex.[5] Tissue-specific hydroxymethylated regions exist in genes encoding transcription factors essential for differentiation, indicating possible roles of 5hmC in related processes.[3] The 5hmC levels on the regulatory regions of genes encoding adipogenic factors increase during development from preadipocytes to mature adipocytes, indicating an association between 5hmC and adipogenesis.[6–10] Since the expression of adipogenic factor genes is highly dynamic during adipogenesis,[11–15] how these genes are affected by 5hmC is worthy of exploration.

Adipose differentiation is a well-studied process by which preadipocytes are converted into mature adipocytes.[16] Key steps in adipose differentiation have been characterized by cell culture studies with established preadipocyte lines, especially 3T3-L1.[13,17,18] The differentiation of 3T3-L1 cells could be induced with a cocktail of insulin, dexamethasone and an agent that activates the cAMP signaling pathway (e.g., methylisobutylxanthine, MIX). cAMP-responsive element-binding protein (CREB) is phosphorylated and activated immediately upon induction.[17] Active CREB initiates the transcription of *Cebpb* which encodes for CCAAT/enhancer-binding protein beta (C/EBPβ),[17,19] a protein that acquires DNA-binding activity after phosphorylation by MAPK and GSK-3β and activates the transcription of *Cebpa* and peroxisome proliferator-activated receptor gamma (*Pparg*) at ∼16 h after the initial cocktail induction[18] which encode for C/EBPα and PPARγ, respectively. C/EBPα and PPARγ transactivate each other in a positive feedback loop[20,21] and function together to activate the expression of adipocyte-specific genes.[22–26] 3T3-L1 preadipocytes overexpressing *Cebpb*,[13] *Cebpa*,[27] or *Pparg* are able to differentiate into mature adipocytes even in the absence of hormone inducers. In addition, mouse embryonic fibroblasts (MEFs) from *Cebpb*$^{-/-}$ mice[28] fail to differentiate into

[1]State Key Laboratory of Cellular Stress Biology, Innovation Center for Cell Signaling Network and Engineering Research Center of Molecular Diagnostics of the Ministry of Education, School of Life Sciences, Xiamen University, Xiamen, Fujian 361100, China
[2]Xiamen Cell Therapy Research Center, the First Affiliated Hospital of Xiamen University, School of Medicine, Xiamen University, Xiamen, Fujian 361003, China
[3]Department of Cardiology, Xiamen Key Laboratory of Cardiac Electrophysiology, Xiamen Institute of Cardiovascular Diseases, The First Affiliated Hospital of Xiamen University, School of Medicine, Xiamen University, Xiamen, China
[4]School of Medicine, Henan Polytechnic University, Jiaozuo, Henan 454000, China
[5]These authors contributed equally
[6]Lead contact
*Correspondence: ghuiling@xmu.edu.cn (H.G.), raissarui@foxmail.com (R.Z.), bali@xmu.edu.cn (B.L.)
https://doi.org/10.1016/j.isci.2023.108312

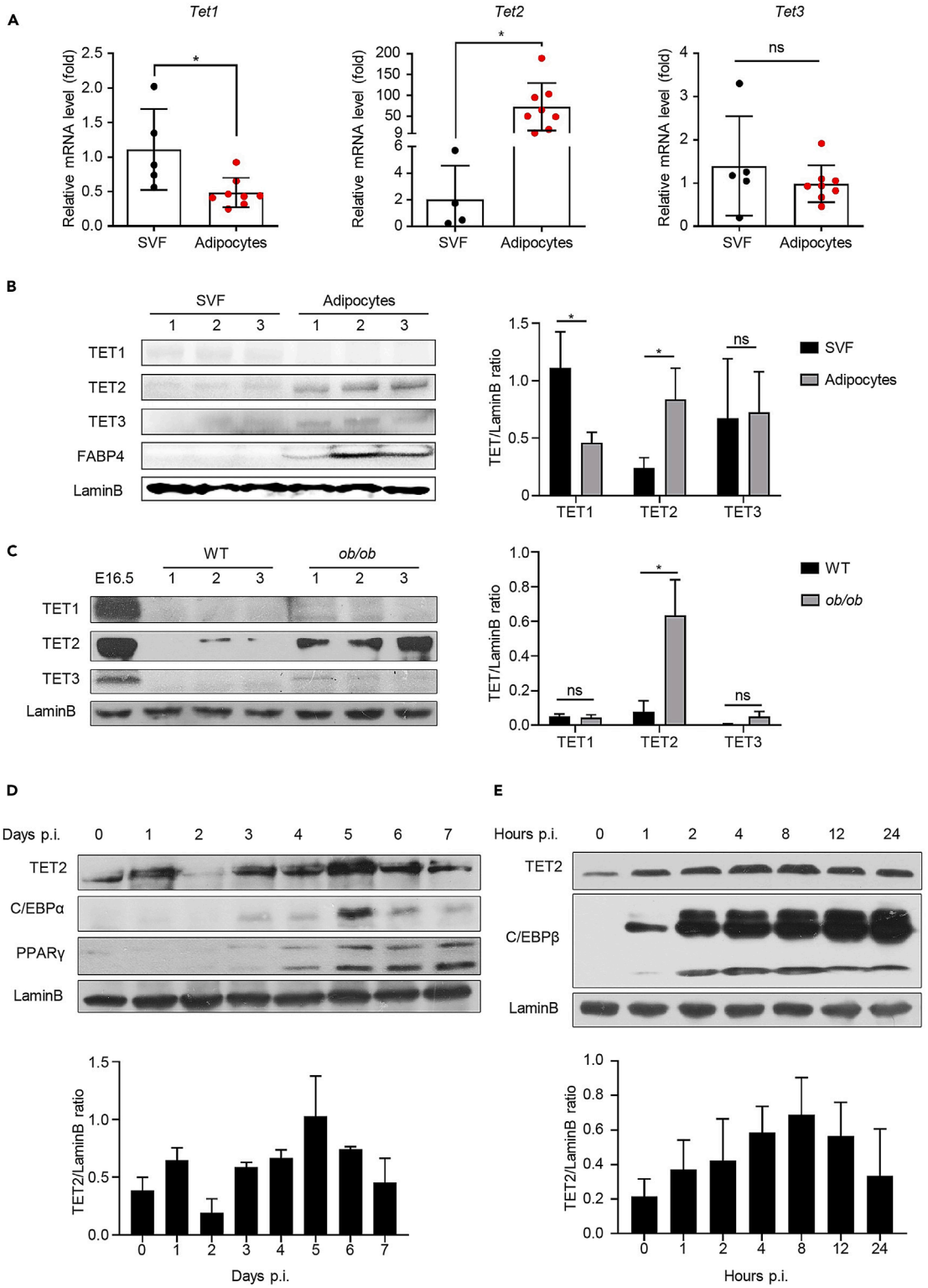

Figure 1. Expression pattern of TET2 in adipose tissues

(A) Relative mRNA levels of TET family proteins in the SVF or mature adipocytes. Both the SVF and the mature adipocytes were purified from iWAT fat pads of 6-week-old mice. RT−qPCR was performed using 18S as the internal control. n = 4~8.

Figure 1. *Continued*

(B) The protein levels of TET family proteins were assessed in the SVF and mature adipocytes from iWAT of 6-week-old mice. FABP4 was used as positive controls for mature adipocytes. The ratio of TET proteins to LaminB was quantified using ImageJ software (right). The numbers 1, 2, and 3 represent three different mice.
(C) The protein levels of TET family proteins in iWAT of WT and *ob/ob* mice at 6 weeks of age were determined by Western blot analysis. Embryonic fibroblasts from wild-type mouse fetuses at embryonic day (E) 16.5 were used as positive controls, and LaminB was used as the loading control. The numbers 1, 2, and 3 represent three different mice. The ratio of TET proteins to LaminB was quantified using ImageJ software (right).
(D and E) 3T3-L1 preadipocytes were treated with MDI for 24 h (E) and 7 days (D). The protein levels of TET2, C/EBPβ, C/EBPα and PPARγ in 3T3-L1 preadipocytes at the indicated times after induction were determined by Western blot analysis. LaminB was used as the loading control. The two lanes of PPARγ represent two isoforms. The three lanes of C/EBPβ represent three isoforms. The protein levels of TET2 at the indicated time points were measured three times independently, and the statistical analysis is presented in the histograms below. The data are presented as the mean ± SD. Statistical analysis was performed using Student's *t* test. *, $p < 0.05$; ns, no significance.

adipocytes, and adipose tissues in *Cebpa*$^{-/-}$[29] mice fail to accumulate lipid droplets. *Pparg*$^{-/-}$ cells failed to develop into adipocytes *in vivo*.[30] In conclusion, the regulation of *Cebpb*, *Cebpa*, and *Pparg* is important for adipocyte differentiation, but whether TET-mediated hydroxymethylation is involved in the early regulation of *Cebpb*, *Cebpa*, and *Pparg* transcription is unclear.

In this study, we found that TET2 expression was significantly higher in adipocytes and plays an essential role in adipogenesis by promoting the expression of *Cebpb*, *Cebpa*, and *Pparg*. TET2 regulated 5hmC levels on the CpG islands (CGIs) of *Cebpb*, *Cebpa*, and *Pparg* at the initial time point of their transcription, which requires the function of CREB. *PdgfRα-cre* mice were crossed with *Tet2*$^{flox/flox}$ mice to generate mice with depletion of *Tet2* in preadipocytes, which inhibited adipocyte enlargement and protected the mice from high-fat diet (HFD)-induced obesity and insulin resistance. All above data claims a vital role of TET2 in adipocyte differentiation.

RESULTS

Tet2 expression is differentially regulated during adipogenesis

To investigate the potential roles of the three TET family members in adipogenesis, we first analyzed the mRNA levels of *Tet1*, *Tet2* and *Tet3* in the stromal vascular fraction (SVF), which contains adipocyte precursors and preadipocytes, and the mature adipocytes purified from inguinal white adipose tissue (iWAT). Quantitative reverse transcription polymerase chain reaction (RT–qPCR) was performed to analyze the mRNA expression patterns. The results showed that in 6-week-old C57BL/6 male mice, the mRNA levels of *Tet2* were upregulated approximately 100-fold in mature adipocytes compared to that of SVF cells, while that of *Tet1* was slightly downregulated and that of *Tet3* remained unchanged (Figure 1A). Consistently, the upregulation of TET2 protein levels in mature adipocytes were most significant among these three proteins (Figure 1B). Moreover, we examined the protein levels of TETs in iWAT from obese *ob/ob* and wild-type mice. Western blotting showed that the expression of TET2 was much higher in the iWAT of *ob/ob* mice compared to that of wild-type mice, and TET2 was the major TET enzyme expressed in iWAT, while TET1 and TET3 were barely detected in the adipose tissues of either mouse strain (Figure 1C). These results suggest a positive association between TET2 and adipogenesis.

To test this hypothesis, we first evaluated the expression profile of TET2 by conducting time course experiments using the methylisobutylxanthine, dexamethasone and insulin (MDI) induction model in 3T3-L1 preadipocytes. Interestingly, we observed two peaks in the expression of TET2 on the first and fifth days after induction (Figure 1D). The expression of TET2 increased after induction, and reached its first peak at 1 day post-induction (p.i.), followed by a decrease to an almost undetectable level on day 2. It then increased again on day 3, and reached a second peak on day 5. Further detection of the TET2 expression levels at more finely divided time points revealed an immediate increase after induction, peaking at 4–8 h and subsequently declining (Figure 1E).

The expression patterns of C/EBPβ, C/EBPα and PPARγ, three key adipogenic factors encoded by adipogenic genes *Cebpb*, *Cebpa*, and *Pparg*,[16] were consistent with previous reports.[16] In this study, we found that C/EBPβ expression increased along with the increasing TET2 expression during the first few hours after induction (Figure 1E), but the expression of C/EBPα and PPARγ were undetectable until day 3, which was the day that the second wave of TET2 expression began (Figure 1D).

Together, these findings demonstrate the dynamic regulation of TET2 during adipogenesis and among different states of adipocytes, implying the possibility of TET2 involvement in the regulation of adipogenesis.

TET2 regulates the transcription of *Cebpb*, *Cebpa*, and *Pparg*

The correlations of expression between TET2 and key regulators raised the hypothesis that TET2 may regulate the transcription of *Cebpb*, *Cebpa*, and *Pparg*. To test this hypothesis, we constructed two stable *Tet2*-knockout 3T3-L1 cell lines via CRISPR/Cas9, i.e., TET2 KO1 and TET2 KO2. The specific target sites of the two guide RNAs are depicted in the schematic diagram (Figure S1A). There was no significant difference in the cell viability between the TET2 KO and control cells during the adipocyte differentiation (Figure S1B).

The MDI cocktail is known to induce expression of several transcription factors, including Kruppel-like factor 4 (*Klf4*) and Krox20 (also known as early growth response gene 2, or *Egr2*). Furthermore, it activates *Creb1* and glucocorticoid receptor (*GR*), which collaborate to activate *Cebpb* and *Cebpd*.[31] It is widely accepted that C/EBPβ and C/EBPδ are responsible for inducing the expression of key adipogenic transcription factors *Cebpa* and *Pparg*, which directly activate the expression of genes associated with adipocyte function.[16,31,32] Hence, the mRNA levels of *Creb1*, *Klf4*, *Egr2*, *Cebpb*, and *Cebpd* were detected at 4 h p.i., while those of *Cebpa* and *Pparg* were detected on day 5 in both *Tet2*-knockout cells and control cells during the adipocyte differentiation. According to the RT–qPCR analysis, the absence of

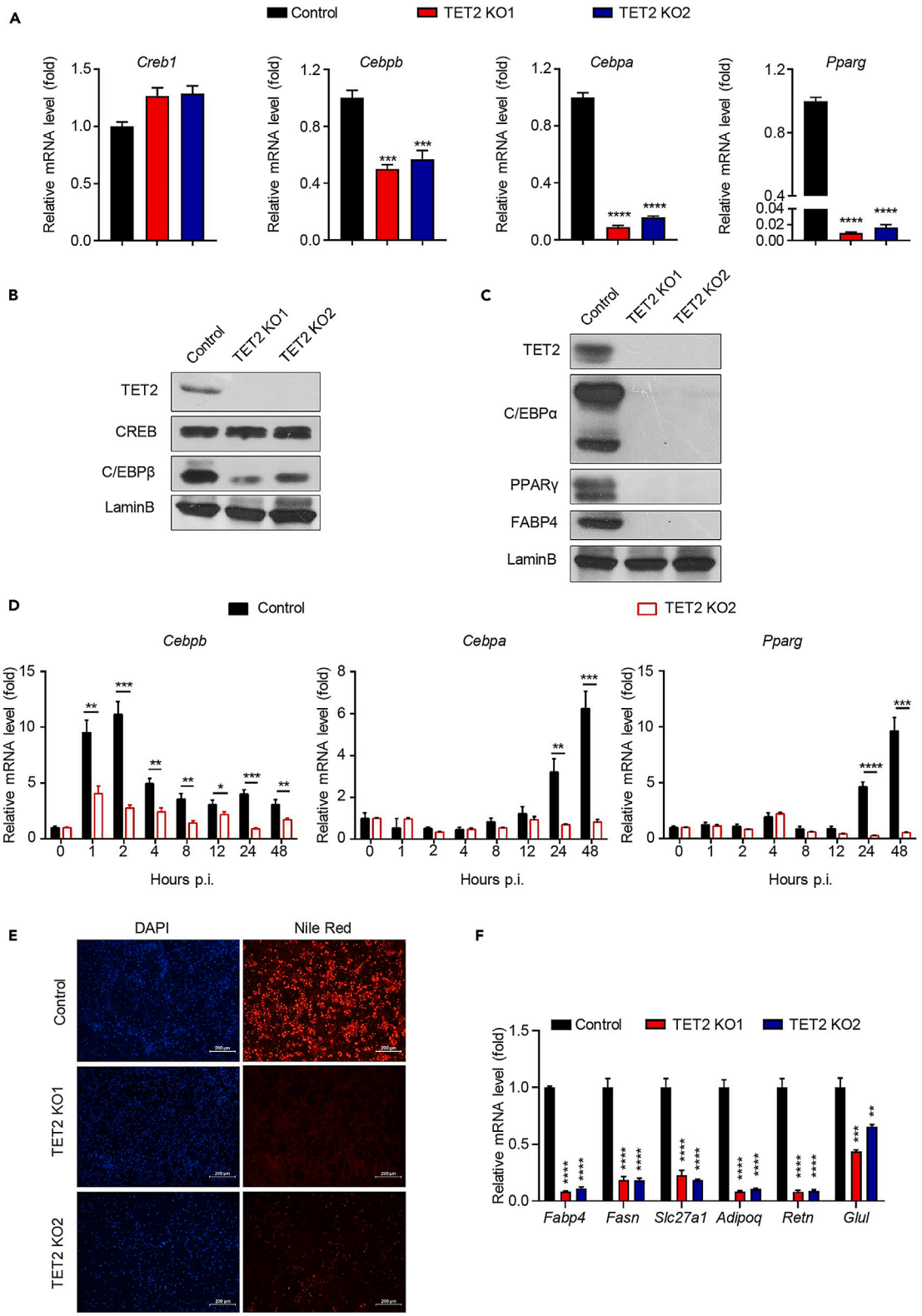
A
Control
TET2 KO1
TET2 KO2
Creb1
Cebpb
Cebpa
Pparg
Relative mRNA level (fold)
B
Control
TET2 KO1
TET2 KO2
TET2
CREB
C/EBPβ
LaminB
C
Control
TET2 KO1
TET2 KO2
TET2
C/EBPα
PPARγ
FABP4
LaminB
D
Control
TET2 KO2
Cebpb
Cebpa
Pparg
Relative mRNA level (fold)
Hours p.i.
E
DAPI
Nile Red
Control
TET2 KO1
TET2 KO2
F
Control
TET2 KO1
TET2 KO2
Relative mRNA level (fold)
Fabp4
Fasn
Slc27a1
Adipoq
Retn
Glul

Figure 2. TET2 is required for the expression of C/EBPβ, C/EBPα and PPARγ

(A) 3T3-L1 cells were infected with lentiviruses expressing sgRNAs targeting *Tet2*, and two single-cell clones were isolated (TET2 KO1 and TET2 KO2). 3T3-L1 preadipocytes infected with lentiviruses expressing an empty vector were used as controls. The mRNA levels of *Creb1* and *Cebpb* at 4 h p.i. and of *Cebpa* and *Pparg* at 5 days p.i. were determined by RT−qPCR.

(B and C) The expression of TET2, CREB and C/EBPβ proteins at 4 h p.i. (C) and the expression of TET2, C/EBPα, PPARγ and FABP4 proteins at 5 days p.i. (D) were determined by Western blot analysis. LaminB was used as the loading control.

(D) *Tet2*-knockout and control 3T3-L1 cells were treated with MDI for 48 h mRNA was extracted at the indicated time points. The mRNA levels of *Cebpb*, *Cebpa*, and *Pparg* were determined by RT−qPCR.

(E) Lipid droplets were stained with Nile Red in control and *Tet2*-knockout 3T3-L1 cells treated with MDI for 7 days. Scale bar, 200 μm.

(F) The mRNA levels of adipocyte-specific genes were determined at 5 days p.i. by RT−qPCR. The data in (A), (D) and (F) are presented as the mean ± SD. Statistical analysis was performed using Student's *t* test. *, $p < 0.05$; **, $p < 0.01$; ***, $p < 0.001$; ****, $p < 0.0001$. See also Figure S1.

TET2 results in an approximate 50% decrease in *Cebpb* mRNA levels and a nearly 90% decrease in *Cebpa* mRNA levels. Moreover, *Pparg* mRNA levels in *Tet2*-knockout cells were only 1% of those observed in the control cells (Figure 2A). However, the transcription of other transcription factors was not affected by *Tet2* knockout (Figures 2A and S1C). Consistently, the protein levels of C/EBPβ, C/EBPα and PPARγ were significantly reduced in *Tet2*-knockout cells (Figures 2B and 2C).

We also constructed a stable TET2-overexpressing 3T3-L1 cell line with lentivirus. However, the mRNA levels of *Cebpb*, *Cebpa*, and *Pparg* were not increased upon TET2 overexpression (Figure S1D). One possible explanation for this observation could be that the endogenous levels of TET2 are already sufficient to facilitate the upregulation of the *Cebpb*, *Cebpa*, and *Pparg* expression during adipogenesis.

To further study the effect of TET2 on the transcriptional kinetics of *Cebpb*, *Cebpa*, and *Pparg* during adipocyte differentiation, we used RT−qPCR to examine the mRNA dynamics of *Cebpb*, *Cebpa*, and *Pparg* in *Tet2*-knockout and control 3T3-L1 preadipocytes (Figures 2D and S1E). The mRNA levels of *Cebpb* increased rapidly within 1 h after induction, while those of *Cebpa* and *Pparg* started to increase at 1 day after induction in the 3T3-L1 control cells. These increases were blunted in *Tet2*-knockout cells, suggesting that the increases in *Cebpb*, *Cebpa*, and *Pparg* mRNA levels require the function of TET2.

Taken together, these results suggest that TET2 promotes the expression of *Cebpb*, *Cebpa*, and *Pparg* during adipocyte differentiation.

TET2 is required for adipocyte differentiation

Since C/EBPα, C/EBPβ and PPARγ are the three key adipogenic factors, and TET2 is required for their expression, experiments were conducted to investigate the impact of *Tet2* knockout on adipocyte differentiation. The extent of adipogenesis was evaluated by assessing lipid droplets accumulation using Nile red staining. Notably, *Tet2*-knockout cells exhibited a marked reduction in the accumulation of lipid droplets compared to control cells (Figure 2E).

To further confirm adipocyte differentiation, we examined the expression of genes that are highly expressed in mature adipocytes and lowly expressed in preadipocytes, including fatty acid-binding protein 4 (*Fabp4*), fatty acid synthase (*Fasn*), fatty acid transport protein 1 (FATP1, also known as *Slc27a1*), which are involved in lipid synthesis and transport. Additionally, we examined the expression of *Adipoq* and *Retn*, which encode adipokines adiponectin and resistin, as well as glutamate-ammonia ligase (*Glul*), involved in glutamine synthesis. The mRNA levels of these genes were significantly decreased in *Tet2*-knockout cells (Figure 2F). Moreover, the protein level of FABP4 was examined, and as expected, it was dramatically reduced in *Tet2*-knockout cells (Figure 2C).

These findings demonstrate the essential role of TET2 in adipocyte differentiation, which is consistent with its involvement in the regulation of *Cebpb*, *Cebpa*, and *Pparg* expression.

TET2 is essential for the 5hmC at the CGIs of *Cebpb*, *Cebpa*, and *Pparg* that promotes the transcription of these genes

If the enzymatic activity of TET2 is involved in the activation of *Cebpb*, *Cebpa*, and *Pparg*, we hypothesized that we would see enrichment of 5hmC within these loci after induction. Considering that TETs prefer 5mC in a CpG context or in CGIs as their substrates,[33] we performed hydroxymethylated DNA immunoprecipitation (hMeDIP) experiments to detect 5hmC levels on the CGIs of *Cebpb*, *Cebpa*, and *Pparg* during adipocyte differentiation. Genomic DNA was extracted from the control and *Tet2*-knockout 3T3-L1 preadipocytes at specified time points, followed by sonication and immunoprecipitation using an antibody specific for 5hmC. A DNA fragment amplified from lambda DNA (λDNA) was added as a spike-in loading control.[34] As depicted in Figures 3A–3C and S2A, the 5hmC levels on the CGIs of *Cebpb* exhibited a significant increase within 1 h after induction, but then rapidly declined to the original level by 2 h p.i. in control cells. The 5hmC levels of *Cebpa* and *Pparg* increased after induction, reaching their peak at 1 day p.i., and gradually decreased thereafter, although they remained higher than the basal levels until 2 days later in control cells. Importantly, the upregulation of 5hmC was abolished in *Tet2*-knockout cells (Figures 3A–3C and S2A), indicating that TET2 plays a regulatory role in modulating the 5hmC levels within the CGIs of *Cebpb*, *Cebpa*, and *Pparg*.

Furthermore, global 5hmC levels measured by dot blot analysis were significantly reduced in *Tet2*-knockout cells compared to control cells (Figure S2B). Conversely, global 5mC was significantly increased in *Tet2*-knockout cells compared to control cells (Figure S2C).

Consistent with the hMeDIP results, chromatin immunoprecipitation (ChIP) analysis further demonstrated a significant increase in TET2 occupancy on the CGIs of *Cebpb* at 1 h and on the CGIs of *Cebpa* and *Pparg* at day 1, compared to the pre-induction levels (Figures 3D–3F). These findings suggest a correlation between the changes in 5hmC mediated by TET2 and the binding of TET2 to these genes.

Collectively, our findings propose that TET2 regulates the 5hmC levels on the CGIs of *Cebpb*, *Cebpa*, and *Pparg*, and these levels are increased during the initial stages of the transcription of these genes.

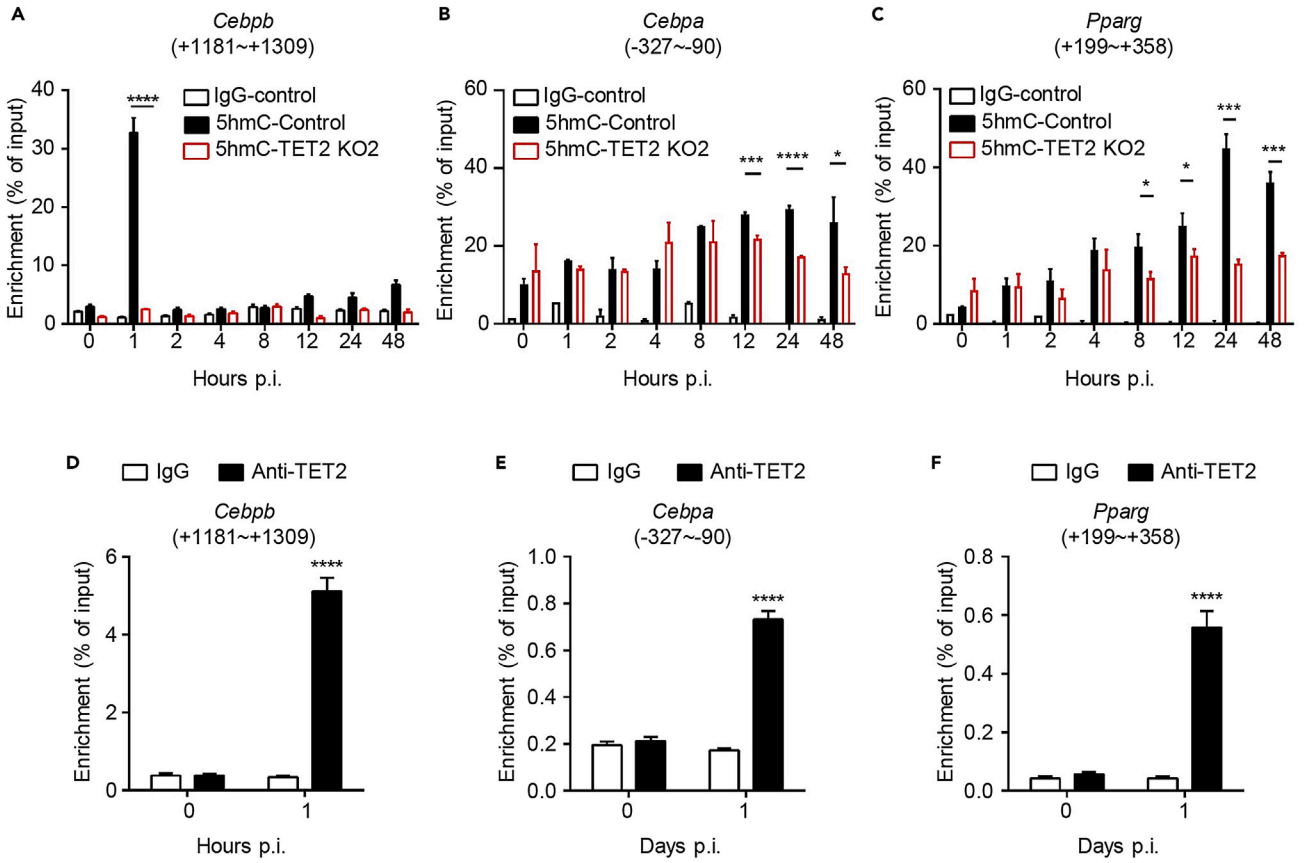

Figure 3. TET2 is essential for 5hmC at the CGIs of *Cebpb*, *Cebpa*, and *Pparg*

(A–C) *Tet2*-knockout and control 3T3-L1 cells were treated with MDI for 48 h. Genomic DNA was extracted at the indicated time points. 5hmC levels at the CGIs of *Cebpb* (A), *Cebpa* (B) and *Pparg* (C) were determined by hMeDIP-qPCR. A fragment amplified from λDNA was added as a spike-in control. The data were normalized to the spike-in control.

(D–F) 3T3-L1 cells were treated with MDI for 1 h (D) and 1 day (E and F). The enrichment of TET2 on the CGIs of *Cebpb* (D), *Cebpa* (E) and *Pparg* (F) was determined before and after induction by ChIP-qPCR assays. The data are presented as the mean ± SD of three biological replicates. Statistical analysis was performed using Student's *t* test. *, $p < 0.05$; ***, $p < 0.001$; ****, $p < 0.0001$. See also Figure S2.

TET2 is recruited to the CpG islands of *Cebpb*, *Cebpa*, and *Pparg* by CREB

We have demonstrated the occupancy of TET2 on the CGIs of *Cebpb*, *Cebpa*, and *Pparg*, but how it is recruited to these specific loci is unclear. Therefore, we sought to determine the protein responsible for recruiting TET2 to regulate 5hmC levels on the CGIs of *Cebpb*, *Cebpa*, and *Pparg*. To identify potential TET2-interacting proteins, we conducted an immunoprecipitation (IP) followed by mass spectrometry (IP-Mass spectrometry) analysis in 3T3-L1 cells stably expressing an FLAG-HA-tagged murine TET2 at 4 h p.i. We identified a large number of potential TET2-interacting proteins, but only CREB and C/EBPβ are known to be associated with adipocyte differentiation (Figure S3A and Table S1).

Considering that more CREB peptides were enriched by FLAG-HA-TET2 according the mass spectrometry analysis, we first focused on CREB, a transcription factor known to regulate the transcription of *Cebpb* during adipocyte differentiation.[19] Our endogenous co-IP results indicated that phospho-CREB could effectively precipitate TET2 at 1 h and 24 h p.i. in 3T3-L1 preadipocytes (Figures 4A and 4B), and the TET2 could also precipitate CREB (Figure S3B), suggesting a potential interaction between CREB and TET2. Then, we assessed whether C/EBPβ was responsible for the recruitment of TET2 since C/EBPβ directly binds to the promoters of *Cebpa* and *Pparg* and can autoregulate its transcription by binding to its own promoter.[35] However, no endogenous association was detected between TET2 and C/EBPβ in 3T3-L1 cells at 24 h after induction (Figure S3C). Additionally, exogenous coIP experiments were performed in HEK293T cells using TET2 and C/EBPβ expression constructs, and no interaction between TET2 and C/EBPβ was observed (Figure S3D). These results suggest that CREB is the major protein responsible for recruitment of TET2 to the CGIs of *Cebpb*, *Cebpa*, and *Pparg*.

TET2 shares a highly conserved C-terminal region and a less conserved N-terminal region with other two TET family members.[36] The C-terminus of TET2 consists of a Cysteine-rich domain and a double stranded β helix domain (DSBH), also known as the CD domain, which constitute the catalytic domain and are essential for enzymatic activities of TET enzymes.[37] To identify the specific CREB binding region within

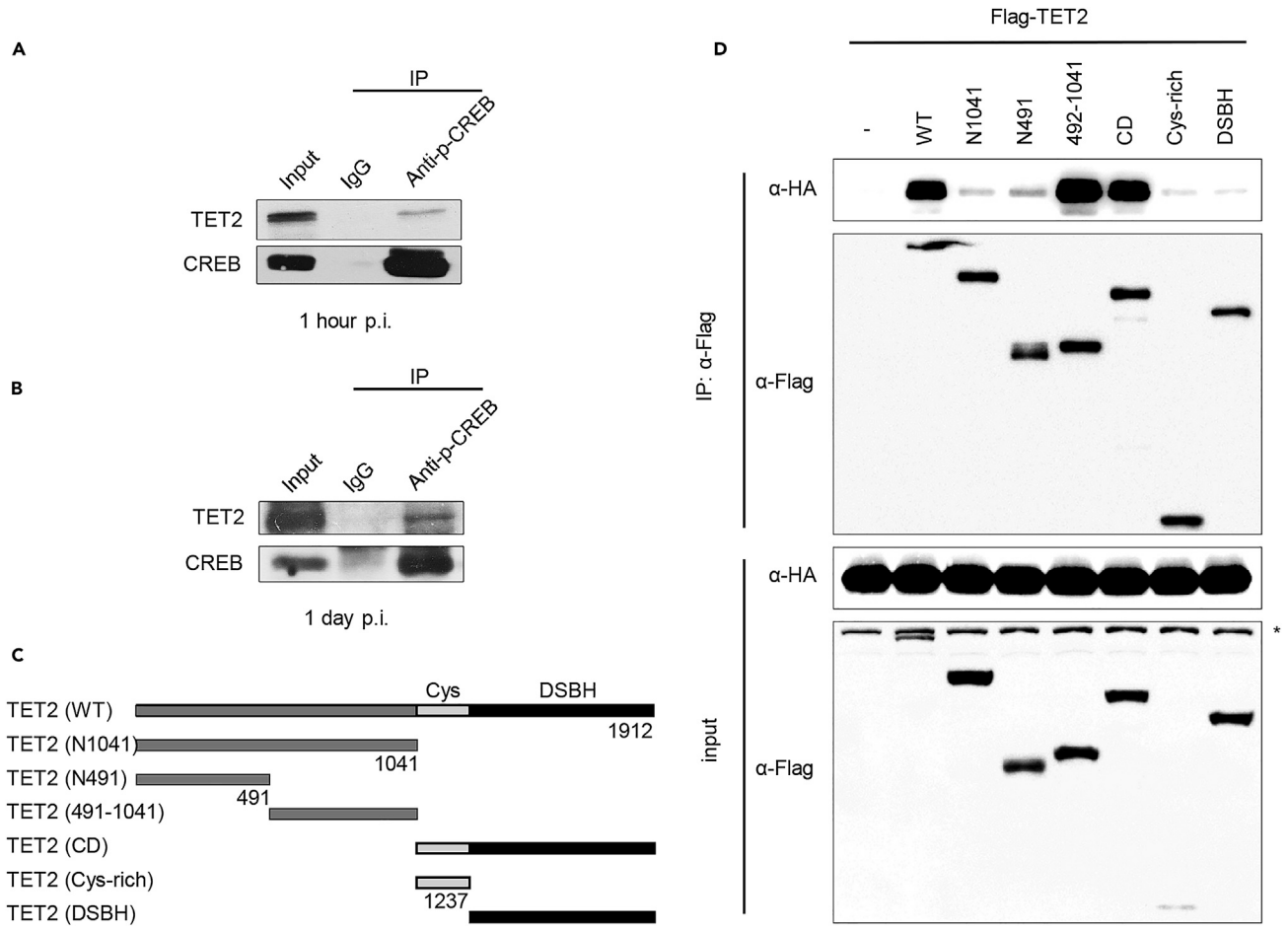

Figure 4. TET2 interacts with CREB

(A and B) 3T3-L1 cells were treated for 1 h (A) and 1 day (B). Cell lysates were prepared and immunoprecipitated with an antibody against phospho-CREB. The endogenous binding of phospho-CREB and TET2 was analyzed by Western blotting.

(C) Schematic representation of FLAG-tagged murine TET2 truncation mutants.

(D) 293T cells were transiently transfected with expression vectors for HA-CREB and a series of FLAG-TET2 fragments. Cell lysates were subjected to IP with magnetic beads covalently coupling with anti-FLAG antibody, followed by Western blotting. *, non-specific banding. See also Figure S3.

TET2, we co-transfected several FLAG-tagged deletion mutants of murine TET2 along with an HA-tagged murine CREB in HEK293T cells and performed Co-IP experiments using an anti-Flag antibody. The results demonstrated a strong interaction between CREB and the CD domain as well as the region 492–1041 of N-terminal, which adjacent to the CD domain of TET2 (Figures 4C and 4D), suggesting that these two regions were required for TET2 to bind CREB protein.

To explore the potential role of CREB in recruiting TET2 to the CGIs of *Cebpb*, *Cebpa*, and *Pparg*, we first sought to determine whether CREB binds to these regions. Through an analysis of putative CREB binding sites within these regions using the JASPAR database, we identified several potential CREB binding sites (Figure S4A). This finding suggests that CREB may possess the ability to bind to the loci of *Cebpb*, *Cebpa*, and *Pparg*. To experimentally validate this hypothesis, we performed ChIP experiments using an anti-CREB antibody in 3T3-L1 preadipocytes. The binding of CREB to these regions was increased after induction (Figure 5A), consistent with the TET2 binding pattern (Figure 3B). Furthermore, publicly available ChIP-seq data (GEO: GSE76619)[38] also demonstrated significant binding of phospho-CREB to these regions (Figure S4C).

Additionally, we identified the loci of *Ebf2*, *Cebpd*, *Klf5* and *Med1* as phospho-CREB binding sites from ChIP-seq data (GEO: GSE76619) (Figure S5A). To address whether these loci could be affected by TET2, we next performed ChIP-qPCR experiments in control and *Tet2*-knockout 3T3-L1 cells. As shown in Figure S5B, TET2 was found to bind to the loci of *Ebf2* and *Cebpd*, while no binding was observed at the loci of *Klf5* and *Med1*. Furthermore, RT-qPCR results indicated that mRNA levels of *Ebf2* were decreased in *Tet2*-knockout cells, while the mRNA levels of *Cebpd*, *Klf5* and *Med1* remained unaffected by TET2 deficiency (Figure S5C). These findings suggest that not all the loci of CREB association in the adipogenesis process are influenced by TET2, and there may be other factors involved in the regulation of these genes.

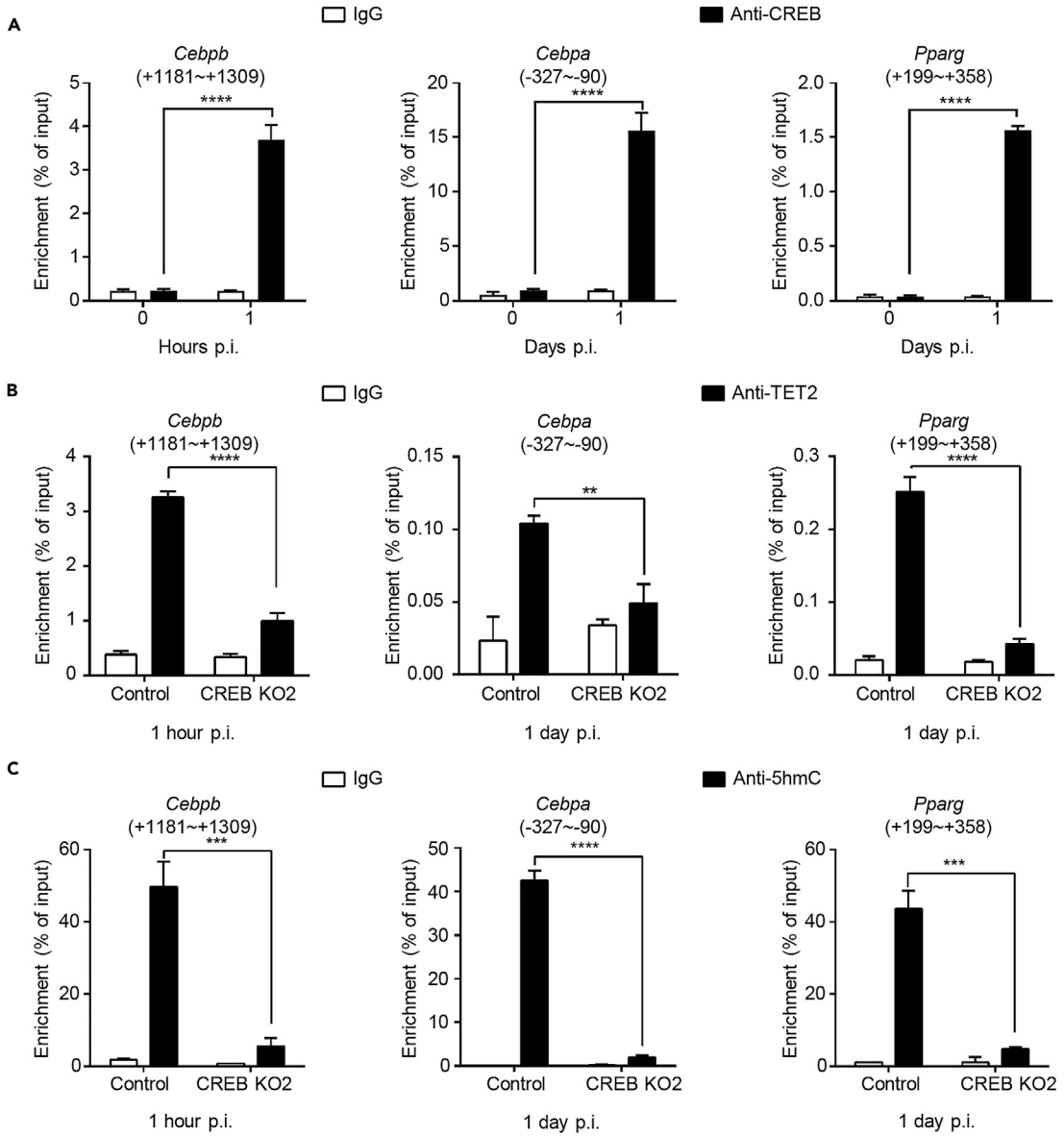

Figure 5. TET2 is recruited to the CGIs of *Cebpb*, *Cebpa*, and *Pparg* by CREB

(A) 3T3-L1 preadipocytes were treated with MDI for 1 h (left) and 1 day (middle and right). The enrichment of CREB on the potential CREB binding sites of *Cebpb* (left), *Cebpa* (middle) and *Pparg* (right) was determined by ChIP-qPCR assays.

(B) *Creb1*-knockout and control 3T3-L1 cells were treated with MDI for 1 h (left) and 1 day (middle and right). The enrichment of TET2 on the CGIs of *Cebpb* (left), *Cebpa* (middle) and *Pparg* (right) was determined by ChIP-qPCR assays.

(C) *Creb1*-knockout and control 3T3-L1 cells were treated with MDI for 1 h (left) and 1 day (middle and right). Genomic DNA was extracted at the indicated time points. The 5hmC levels at the CGIs of *Cebpb* (left), *Cebpa* (middle) and *Pparg* (right) were determined by hMeDIP-qPCR assays. A fragment amplified from λDNA was added as a spike-in control. The data were normalized to the spike-in control. The data are presented as the mean ± SD of three biological replicates. Statistical analysis was performed using Student's *t* test. **, $p < 0.01$; ***, $p < 0.001$; ****, $p < 0.0001$. See also Figures S4 and S5.

To validate whether CREB is essential for TET2 recruitment to the CGIs of *Cebpb*, *Cebpa*, and *Pparg*, we generated stable *Creb1*-knockout 3T3-L1 cell lines via CRISPR/Cas9 (Figure S4B) and performed ChIP assays using an anti-TET2 antibody. The results demonstrated a significant reduction in TET2 enrichment on the CGIs of *Cebpb*, *Cebpa*, and *Pparg* upon CREB depletion (Figure 5B). Furthermore, to assess the impact of CREB on the 5hmC levels within the CGIs of *Cebpb*, *Cebpa*, and *Pparg*, we performed hMeDIP-qPCR experiments in control and *Creb1*-knockout cells. The results showed a reduction in the 5hmC levels on these regions in *Creb1*-knockout cells at the initial stage of transcription (Figure 5C). Taken together, these results suggest that CREB plays a critical role in recruiting TET2 to the CGIs of *Cebpb*, *Cebpa*, and *Pparg*, thereby regulating their 5hmC levels and expression.

Mice with TET2 deficiency in preadipocytes show a significant decrease in adipogenesis and resistance to diet-induced obesity

In vitro studies have demonstrated that TET2 deficiency inhibits adipocyte differentiation, so we aimed to further investigate the role of TET2 in adipogenesis *in vivo*. *PdgfRα-Cre* directs recombination in the vast majority of adipose precursor cells (APCs).[39,40] We generated mice in which TET2 was conditionally depleted in APCs by *PdgfRα-Cre*. The resulting *PdgfRα-Cre;Tet2*$^{flox/flox}$ mice are henceforth referred as *Tet2*$^{PdgfR\alpha-/-}$ mice. Littermates lacking the *Cre* gene (*Tet2*$^{flox/flox}$) were used as wild-type controls. *Tet2*$^{PdgfR\alpha-/-}$ mice pups were obtained at the expected Mendelian ratio, and all survived beyond 6 weeks after birth without any obvious development defects (Figures S6A–S6C). The food and water intake, the movement and the size of adipose tissues in control and *Tet2*$^{PdgfR\alpha-/-}$ mice were also comparable (Figures S6D and S6E).

To confirm the successful downregulation of *Tet2* in adipocyte precursors, we examined mRNA levels of *Tet2* in mature adipocytes from iWAT of control and *Tet2*$^{PdgfR\alpha-/-}$ mice. The results demonstrated a dramatically reduction in the expression of *Tet2* mRNA in the adipocytes of *Tet2*$^{PdgfR\alpha-/-}$ mice, indicating effective knockout of *Tet2* in the adipocyte precursors from which these mature adipocytes originated (Figure 6A). We also examined the expression levels of *Cebpb*, *Cebpa*, and *Pparg*, and found that their mRNA levels were also significantly reduced in *Tet2*$^{PdgfR\alpha-/-}$ mice (Figure 6A). Furthermore, we assessed mRNA levels of *Fabp4*, *Fasn*, *Slc27a1*, *Adipoq*, *Retn*, and *Lep*, which encode proteins involved in adipocyte function. While the mRNA levels of *Lep* remained unchanged, the mRNA levels of all the other genes were significantly reduced in *Tet2*$^{PdgfR\alpha-/-}$ mice (Figure 6A).

Since the body weight showed no significant differences between control and *Tet2*$^{PdgfR\alpha-/-}$ mice until 14 weeks of age fed a normal diet chow (NCD) (Figure S7A), to investigate the impact of TET2 depletion in adipose precursor cells on adipogenesis, we administered high fat diet (HFD) (60% calories from fat) to these two groups from 3 weeks of age. The body weights of the two groups began to significantly diverge after 8 weeks of HFD feeding (Student's *t* test: $p = 0.0001$), with *Tet2*$^{PdgfR\alpha-/-}$ mice gaining less weight on the HFD (Figure 6B), as mirrored by the smaller body size of *Tet2*$^{PdgfR\alpha-/-}$ mice (Figure 6C). Body composition analysis showed decreased fat mass and fat percentage but not lean mass in *Tet2*$^{PdgfR\alpha-/-}$ mice (Figure 6D). These differences were also mirrored by the decreased volumes of iWAT and epididymal WAT (eWAT) depots in *Tet2*$^{PdgfR\alpha-/-}$ mice (Figure 6E). H&E staining of iWAT and eWAT sections revealed a significant decrease in adipocyte volume in the *Tet2*-deficient fat depots (Figure 6F). These findings suggest that the depletion of TET2 in adipose precursor cells in mice leads to the downregulation of adipogenic genes and inhibits the enlargement of mature adipocytes under high-fat diet conditions.

To further confirm that the impairment of adipocyte is due to the loss of TET2 in adipocyte precursors, we isolated the SVF cells from iWAT of control and *Tet2*$^{PdgfR\alpha-/-}$ mice for *in vitro* culture. The 5hmC levels on the CGIs of *Cebpb*, *Cebpa*, and *Pparg* were reduced significantly in the *Tet2*$^{PdgfR\alpha-/-}$ group (Figure S7B). Then Oil red staining was performed to visualize lipid droplets on day 7 after induction. The results demonstrated a significant reduction in the accumulation of lipid droplets in the *Tet2*$^{PdgfR\alpha-/-}$ group compared to the control group (Figure S7C).

Since high-fat diet induced obesity may cause ectopic fat deposition and exert some unfavorable metabolic modulations, first, the livers of both genotypes were isolated and subjected to histologic section and H&E staining. We found that the lipid accumulation was largely reduced in livers of *Tet2*$^{PdgfR\alpha-/-}$ mice (Figure S8A), while the levels of alanine aminotransferase (ALT) and aspartate aminotransferase (AST) were not changed (Figure S8B). Moreover, the levels of total cholesterol were significant reduced in *Tet2*$^{PdgfR\alpha-/-}$ mice compared to the control mice, although there were no significant differences in other blood markers (Figure S8C). In addition, the *Tet2*$^{PdgfR\alpha-/-}$ mice demonstrated improved glucose tolerant and insulin sensitive than controls (Figure S8D).

Collectively, these data indicate that depletion of TET2 in adipose precursor cells in mice leads to the downregulation of adipogenic genes and inhibits the enlargement of mature adipocytes during HFD induced obesity.

DISCUSSION

5hmC is an epigenetic modification that plays a crucial role in regulating the transcription of genes involved in development and differentiation. Previous studies have explored the role of TET family proteins, responsible for "writing" 5hmC, in adipogenesis.[8,10] Y Yoo and his colleagues[8] have demonstrated that *Tet1* and *Tet2* knockdown impaired the lipid droplet accumulation in differentiated 3T3-L1 cells. They also exhibited a downregulation of *Pparg* transcription upon *Tet2* knockdown. However, the underlying mechanism through which TET family proteins facilitate *Pparg* expression remained unclear. In this study, we provide compelling evidence showing a positive correlation between TET2-mediated 5hmC and the transcription of key transcription factors during the early stage of adipogenesis. We observed a significant increase of TET2 expression in response to adipocyte differentiation induction. Moreover, depletion of TET2 both *in vitro* and *in vivo* impedes adipogenesis by blocking the expression of *Cebpb*, *Cebpa*, and *Pparg* during the early stage of adipocyte differentiation. Further investigation found that TET2-mediated 5hmC upregulation on the CGIs of the three genes occurs at the initial of their transcription. In addition, we identified CREB as a crucial factor responsible for recruiting TET2 to regulate the 5hmC of these genes, providing valuable insights into the mechanism underlying 5hmC formation during adipogenesis.

5hmC is an epigenetic modification that positively regulates gene expression.[2–4] Existing evidence suggests that 5hmC may play a role in transcription by remodeling and organizing the chromatin structure. For instance, methyl-CpG-binding protein 2 (MeCP2) binds to 5hmC-enriched regions, facilitating the chromatin accessibility.[2] Additionally, the Nucleosome Remodeling and Deacetylase (NURD) complex containing MBD3 preferentially binds to 5hmC, and antagonizes the ATP-dependent nucleosome remodeling complex to regulate the transcription of 5hmC-marked genes.[41] Considering that TET2 is a "writer" of 5hmC, we sought to investigate whether TET2 regulates these genes via 5hmC. Herein, we observed a synchronous increase in TET2-mediated 5hmC along with the gene expression of *Cebpb, Cebpa, and Pparg*.

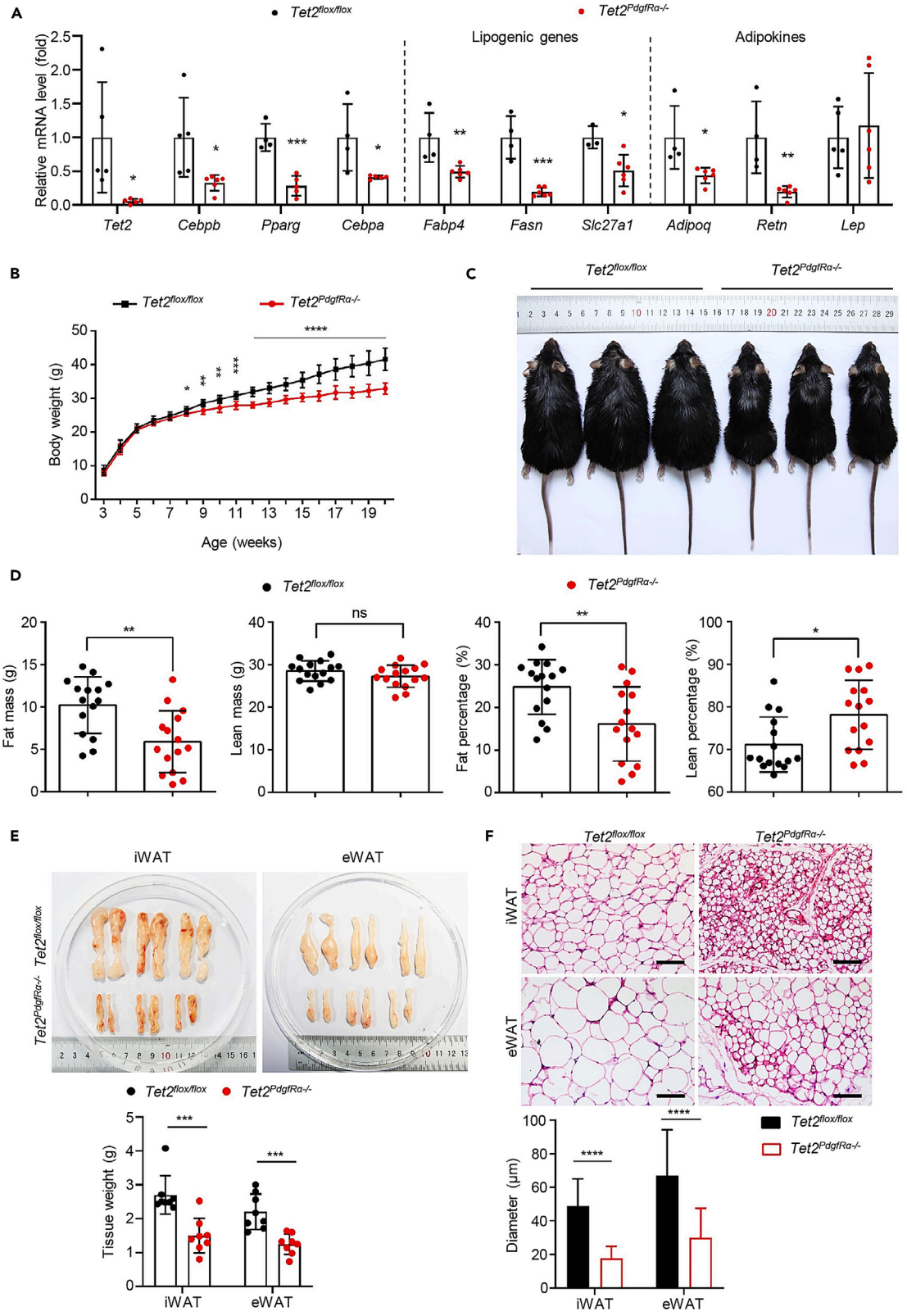
A
Tet2flox/flox
Tet2PdgfRα-/-
Lipogenic genes
Adipokines
Relative mRNA level (fold)
Tet2
Cebpb
Pparg
Cebpa
Fabp4
Fasn
Slc27a1
Adipoq
Retn
Lep
B
Body weight (g)
Age (weeks)
C
D
Fat mass (g)
Lean mass (g)
Fat percentage (%)
Lean percentage (%)
ns
E
iWAT
eWAT
Tissue weight (g)
F
Diameter (μm)

Figure 6. Mice with TET2 deficiency in preadipocytes show a significant decrease in adipogenesis and resistance to diet-induced obesity

(A) The mRNA levels of *Tet2* and the three key transcription factor genes *Cebpb*, *Cebpa*, *Pparg*, as well as lipogenic genes and genes encoding adipokines were analyzed by qPCR in mature adipocytes isolated from iWAT of 6-week-old C57BL/6 mice (n = 5).

(B and C) Growth curves of body weight (B) and a representative image (C) of $Tet2^{flox/flox}$ and $Tet2^{PdgfR\alpha-/-}$ mice fed an HFD (n = 8).

(D) Fat mass, lean mass, and their ratios to body weight were analyzed in $Tet2^{flox/flox}$ and $Tet2^{PdgfR\alpha-/-}$ mice fed an HFD for 17 weeks by EchoMRI (n = 15).

(E) Representative images of iWAT and eWAT (upper) and the tissue weight (lower) in 22-week-old $Tet2^{flox/flox}$ and $Tet2^{PdgfR\alpha-/-}$ mice fed an HFD.

(F) Representative H&E staining images of iWAT and eWAT from 22-week-old $Tet2^{flox/flox}$ and $Tet2^{PdgfR\alpha-/-}$ mice fed an HFD. Scale bar, 100 μm. The histograms below represent the average diameters of adipocytes in each group. The data are presented as the mean ± SD of three biological replicates. Student's *t* test, *, $p < 0.05$, **, $p < 0.01$; ns, no significance. See also Figures S6–S8.

Moreover, depletion of TET2 blunted the upregulation of 5hmC levels in the loci of these genes induced by adipogenic differentiation cocktail and decreased their mRNA levels. In addition, 5mC is an epigenetic modification known to repress gene expression either by recruiting proteins involved in gene repression[42–46] or by inhibiting the binding of transcription factor(s) to DNA.[47] 5mC is converted by TET family proteins to 5hmC and further to 5-formylcytosine (5fC) and 5-carboxylcytosine (5caC), which can be removed by base excision repair (BER) pathway. Therefore, 5hmC also serves as an intermediate in the process of 5mC removement. A previous study has elucidated the pivotal role of another 5hmC "writer" TET3 in adipogenesis.[10] TET3 is recruited by C/EBPδ to promote the expression of adipogenic genes via removing 5mC. Within our study, we have revealed that TET2 is recruited by another transcription factor CREB to facilitate the 5hmC levels on *Cebpb, Cebpa, and Pparg* loci. Due to the distinct distribution of CREB binding sites and C/EBP motifs, the collaboration between TET2 and TET3 enables the regulation of a broader spectrum of gene expression. Moreover, their binding to target loci occurs at varying time points. The enrichment of TET3 on the locus of *Pparg* peaks before induction (D0), whereas TET2 binds to the *Pparg* locus at a later time point (D1). TET3 binds to the locus of *Adipoq* at 2 days post-induction, a time point at which TET2 protein levels were barely detectable. The temporal and spatial complementarity between TET2 and TET3 enables a finely orchestrated manipulation of gene expression during the process of adipocyte differentiation.

TET2 can also facilitate the transcription activity in a catalytic-independent manner. For instance, TET2 enhances the association between O-GlcNAc transferase (OGT) and Host Cell Factor 1 (HCF1) and facilitates the glycosylation modification of the latter, a component of SET1/COMPASS, thereby promoting SET1/COMPASS-mediated trimethylation of H3K4,[48] which is positively correlated with gene activation.[31,48] Our study confirmed the interaction between OGT and TET2 by IP-mass spectrometry analysis. However, we did not detect any interaction between TET2 and any of the components of SET1/COMPASS complex at 4 h after induction. Hence, we can exclude the involvement of this mechanism in the early stage of adipocyte differentiation.

Most studies on the role of CREB in adipogenesis have focused on its function as a transcription factor. A previous study has reported that knockdown of *Creb1*, along with its closely related factor *Atf1*, resulted in a moderate reduction in *Cebpb* expression and a substantial reduction in both *Cebpa* and *Pparg* expression.[49] These findings align with the expression patterns observed in *Tet2*-knockout cells, prompting our interest in exploring whether the diminished expression of the three genes upon *Tet2* knockout could be attributed to disruptions in *Creb1* expression or CREB binding to these target genes. However, our data showed that the expression level of *Creb1* and the occupancy of CREB on chromatin (data not shown) were not impaired upon TET2 knockout, ruling out this possibility. Instead, our study proposes another role of CREB in modulating 5hmC levels on the loci of *Cebpb*, *Cebpa*, and *Pparg*, providing new insights into the mechanism by which CREB regulates the expression of *Cebpa* and *Pparg* during adipogenesis.

To further validate the mechanism *in vivo*, we used a $Tet2^{PdgfR\alpha-/-}$ mouse model in which *Tet2* is conditionally knocked-out in APCs. This enables a focused exploration of TET2' influence on adipogenesis, particularly within the context of adipocyte differentiation. Our observations revealed a significant reduction in both the adipose tissue size and adipocyte dimensions in $Tet2^{PdgfR\alpha-/-}$ mice fed an HFD. To further validate the contribution of TET2 deficiency to this phenotype, we isolated primary SVF cells from iWAT of both control and $Tet2^{PdgfR\alpha-/-}$ mice. Both the 5hmC levels on the CGIs of *Cebpb*, *Cebpa*, and *Pparg* and their mRNA levels as well as other adipogenic genes were significantly decreased. Furthermore, upon standard MDI induction, lipid droplet accumulation was notably diminished in the $Tet2^{PdgfR\alpha-/-}$ group. Collectively, these findings robustly validate the pivotal role of TET2 in adipocyte differentiation. Furthermore, the leaner *Tet2* conditional mice fed an HFD exhibited enhanced insulin sensitivity than control mice, emphasizing the impact of TET2 on HFD-induced obesity.

In conclusion, our study further clarifies the important role of TET2 in adipocyte differentiation and elucidates a mechanism by which TET2 regulates gene expression during adipocyte differentiation, providing a potential target for obesity treatment.

Limitations of the study

In our study, we have successfully demonstrated a positive correlation between the upregulation of 5hmC and the initiation of transcription for the three adipogenic transcription factor genes. This provides the basis for proposing a mechanism that TET2 regulates these genes via 5hmC. However, it's important to acknowledge that direct evidence supporting this mechanism is lacking. This gap exists because the specific "reader(s)" responsible for recognizing 5hmC and exerting the regulation of transcription in this process have not been identified. This needs further exploration in the future.

Furthermore, the *Pdgfra*-Cre can also target other cell types, such as glial cells,[50] in which TET2 is also highly expressed.[51] Despite this caveat, it is currently the most widely used Cre transgenic mouse tool that targets preadipocytes. To validate the importance of TET2 in adipogenic differentiation of preadipocytes, we isolated primary SVF cells to perform *in vitro* adipocyte differentiation induction, and observed

reduced lipid droplet accumulation in *Tet2*-knockout group. However, the potential impact of *Tet2* deficiency in other cell types on the lean phenotype and physiological indices in $Tet2^{PdgfR\alpha-/-}$ mice cannot be completely rule out.

STAR★METHODS

Detailed methods are provided in the online version of this paper and include the following:

- KEY RESOURCES TABLE
- RESOURCE AVAILABILITY
  - Lead contact
  - Materials availability
  - Data and code availability
- EXPERIMENTAL MODEL AND STUDY PARTICIPANTS DETAILS
  - Cell lines
  - Mice
- METHOD DETAILS
  - Isolation of adipose SVF and mature adipocytes
  - Quantitative reverse transcription PCR
  - Western blot analysis
  - Cell-counting-kit-8 (CCK-8) assay
  - Nile red staining
  - Plasmids, lentivirus production and lentivirus-mediated gene transfer
  - hMeDIP
  - ChIP
  - Co-IP
  - IP-mass spectrometry
  - Body weight, body composition
  - Food and water intake and movement measurements
  - Hematoxylin and eosin (H&E) staining
  - Blood analysis
  - Glucose tolerance test (GTT)
  - Insulin tolerance test (ITT)
- QUANTIFICATION AND STATISTICAL ANALYSIS

SUPPLEMENTAL INFORMATION

Supplemental information can be found online at https://doi.org/10.1016/j.isci.2023.108312.

ACKNOWLEDGMENTS

This work was supported by grants from the Key R & D Project of the Ministry of Science and Technology (2020YFA0112301 to B-A.L.), the National Natural Science Foundation of China (grant number 81972458 to B-A.L., 32071150 to H.G., 82103092 to R.Z., and 81700775 to S-N.L.), the Natural Science Foundation of Fujian Province (grant number 2022J05312 to R.Z.), Project of Xiamen Cell Therapy Research, Xiamen, Fujian, China (Grant No. 3502Z20214001), the Health-Education Joint Research Project of Fujian Province (grant numbers 2019-WJ-34 to B-A.L. and Z-M.Z.), and "Project 111" sponsored by the State Bureau of Foreign Experts and Ministry of Education (grant number B06016).

AUTHOR CONTRIBUTIONS

Y-J.L. designed and carried out the overall experiments and wrote the paper. T.H., Z-F.L., and Z.S. performed the experiments and analyzed and interpreted the data. S.W., H-M.S., L-F.H., Y-X.W., and C.Z. assisted with mouse experiments and data analysis. B-Z.Z. and S-N.L. (Shanni Li) assisted with plasmid construction. B-A.L., H-L.G., R.Z., and S-N.L. (Shengnan Li) supervised the project and revised the manuscript. B-A.L. is the guarantor of this work and, as such, had full access to all the data in the study and takes responsibility for the integrity of the data and the accuracy of the data analysis.

DECLARATION OF INTERESTS

The authors declare no competing or financial interests.

INCLUSION AND DIVERSITY

We support inclusive, diverse, and equitable conduct of research.

Received: December 2, 2022
Revised: August 10, 2023
Accepted: October 20, 2023
Published: October 23, 2023

REFERENCES

1. Tahiliani, M., Koh, K.P., Shen, Y., Pastor, W.A., Bandukwala, H., Brudno, Y., Agarwal, S., Iyer, L.M., Liu, D.R., Aravind, L., and Rao, A. (2009). Conversion of 5-methylcytosine to 5-hydroxymethylcytosine in mammalian DNA by MLL partner TET1. Science *324*, 930–935. https://doi.org/10.1126/science.1170116.
2. Mellén, M., Ayata, P., Dewell, S., Kriaucionis, S., and Heintz, N. (2012). MeCP2 binds to 5hmC enriched within active genes and accessible chromatin in the nervous system. Cell *151*, 1417–1430. https://doi.org/10.1016/j.cell.2012.11.022.
3. He, B., Zhang, C., Zhang, X., Fan, Y., Zeng, H., Liu, J., Meng, H., Bai, D., Peng, J., Zhang, Q., et al. (2021). Tissue-specific 5-hydroxymethylcytosine landscape of the human genome. Nat. Commun. *12*, 4249. https://doi.org/10.1038/s41467-021-24425-w.
4. Ficz, G., Branco, M.R., Seisenberger, S., Santos, F., Krueger, F., Hore, T.A., Marques, C.J., Andrews, S., and Reik, W. (2011). Dynamic regulation of 5-hydroxymethylcytosine in mouse ES cells and during differentiation. Nature *473*, 398–402. https://doi.org/10.1038/nature10008.
5. Globisch, D., Münzel, M., Müller, M., Michalakis, S., Wagner, M., Koch, S., Brückl, T., Biel, M., and Carell, T. (2010). Tissue distribution of 5-hydroxymethylcytosine and search for active demethylation intermediates. PLoS One *5*, e15367. https://doi.org/10.1371/journal.pone.0015367.
6. Sérandour, A.A., Avner, S., Oger, F., Bizot, M., Percevault, F., Lucchetti-Miganeh, C., Palierne, G., Gheeraert, C., Barloy-Hubler, F., Péron, C.L., et al. (2012). Dynamic hydroxymethylation of deoxyribonucleic acid marks differentiation-associated enhancers. Nucleic Acids Res. *40*, 8255–8265. https://doi.org/10.1093/nar/gks595.
7. Fujiki, K., Shinoda, A., Kano, F., Sato, R., Shirahige, K., and Murata, M. (2013). PPAR gamma-induced PARylation promotes local DNA demethylation by production of 5-hydroxymethylcytosine. Nat. Commun. *4*, 2262. https://doi.org/10.1038/ncomms3262.
8. Yoo, Y., Park, J.H., Weigel, C., Liesenfeld, D.B., Weichenhan, D., Plass, C., Seo, D.G., Lindroth, A.M., and Park, Y.J. (2017). TET-mediated hydroxymethylcytosine at the Pparγ locus is required for initiation of adipogenic differentiation. Int. J. Obes. *41*, 652–659. https://doi.org/10.1038/ijo.2017.8.
9. Dubois-Chevalier, J., Oger, F., Dehondt, H., Firmin, F.F., Gheeraert, C., Staels, B., Lefebvre, P., and Eeckhoute, J. (2014). A dynamic CTCF chromatin binding landscape promotes DNA hydroxymethylation and transcriptional induction of adipocyte differentiation. Nucleic Acids Res. *42*, 10943–10959. https://doi.org/10.1093/nar/gku780.
10. Park, J., Lee, D.H., Ham, S., Oh, J., Noh, J.R., Lee, Y.K., Park, Y.J., Lee, G., Han, S.M., Han, J.S., et al. (2022). Targeted erasure of DNA methylation by TET3 drives adipogenic reprogramming and differentiation. Nat. Metab. *4*, 918–931. https://doi.org/10.1038/s42255-022-00597-7.
11. Cao, Z., Umek, R.M., and McKnight, S.L. (1991). Regulated expression of three C/EBP isoforms during adipose conversion of 3T3-L1 cells. Genes Dev. *5*, 1538–1552. https://doi.org/10.1101/gad.5.9.1538.
12. Macdougald, O.A., and Lane, M.D. (1995). Transcriptional regulation of gene expression during adipocyte differentiation. Annu. Rev. Biochem. *64*, 345–373. https://doi.org/10.1146/annurev.bi.64.070195.002021.
13. Yeh, W.C., Cao, Z., Classon, M., and McKnight, S.L. (1995). Cascade regulation of terminal adipocyte differentiation by 3 members of the C/EBP family of leucine-zipper proteins. Genes Dev. *9*, 168–181. https://doi.org/10.1101/gad.9.2.168.
14. Lane, M.D., Tang, Q.Q., and Jiang, M.S. (1999). Role of the CCAAT enhancer binding proteins (C/EBPs) in adipocyte differentiation. Biochem. Biophys. Res. Commun. *266*, 677–683.
15. He, T., Wang, S., Li, S., Shen, H., Hou, L., Liu, Y., Wei, Y., Xie, F., Zhang, Z., Zhao, Z., et al. (2023). Suppression of preadipocyte determination by SOX4 limits white adipocyte hyperplasia in obesity. iScience *26*, 106289. https://doi.org/10.1016/j.isci.2023.106289.
16. Tang, Q.Q., and Lane, M.D. (2012). Adipogenesis: from stem cell to adipocyte. Annu. Rev. Biochem. *81*, 715–736. https://doi.org/10.1146/annurev-biochem-052110-115718.
17. Zhang, J.W., Klemm, D.J., Vinson, C., and Lane, M.D. (2004). Role of CREB in transcriptional regulation of CCAAT/enhancer-binding protein beta gene during adipogenesis. J. Biol. Chem. *279*, 4471–4478. https://doi.org/10.1074/jbc.M311327200.
18. Tang, Q.Q., and Lane, M.D. (1999). Activation and centromeric localization of CCAAT/enhancer-binding proteins during the mitotic clonal expansion of adipocyte differentiation. Genes Dev. *13*, 2231–2241. https://doi.org/10.1101/gad.13.17.2231.
19. Niehof, M., Manns, M.P., and Trautwein, C. (1997). CREB controls LAP/C/EBP beta transcription. Mol. Cell Biol. *17*, 3600–3613. https://doi.org/10.1128/mcb.17.7.3600.
20. Clarke, S.L., Robinson, C.E., and Gimble, J.M. (1997). CAAT/enhancer binding proteins directly modulate transcription from the peroxisome proliferator-activated receptor gamma 2 promoter. Biochem. Biophys. Res. Commun. *240*, 99–103. https://doi.org/10.1006/bbrc.1997.7627.
21. Wu, Z., Rosen, E.D., Brun, R., Hauser, S., Adelmant, G., Troy, A.E., McKeon, C., Darlington, G.J., and Spiegelman, B.M. (1999). Cross-regulation of C/EBP alpha and PPAR gamma controls the transcriptional pathway of adipogenesis and insulin sensitivity. Mol. Cell *3*, 151–158. https://doi.org/10.1016/s1097-2765(00)80306-8.
22. Graves, R.A., Tontonoz, P., and Spiegelman, B.M. (1992). Analysis of a tissue-specific enhancer: ARF6 regulates adipogenic gene expression. Mol. Cell Biol. *12*, 1202–1208. https://doi.org/10.1128/mcb.12.3.1202.
23. Tontonoz, P., Hu, E., Graves, R.A., Budavari, A.I., and Spiegelman, B.M. (1994). mPPAR-gamma-2: tissue-specific regulator of an adipocyte enhancer. Genes Dev. *8*, 1224–1234. https://doi.org/10.1101/gad.8.10.1224.
24. Christy, R.J., Yang, V.W., Ntambi, J.M., Geiman, D.E., Landschulz, W.H., Friedman, A.D., Nakabeppu, Y., Kelly, T.J., and Lane, M.D. (1989). Differentiation-induced gene expression in 3T3-L1 preadipocytes: CCAAT/enhancer binding protein interacts with and activates the promoters of two adipocyte-specific genes. Genes Dev. *3*, 1323–1335. https://doi.org/10.1101/gad.3.9.1323.
25. Kaestner, K.H., Christy, R.J., and Lane, M.D. (1990). Mouse insulin-responsive glucose transporter gene: characterization of the gene and trans-activation by the CCAAT/enhancer binding protein. Proc. Natl. Acad. Sci. USA *87*, 251–255. https://doi.org/10.1073/pnas.87.1.251.
26. Kershaw, E.E., Schupp, M., Guan, H.-P., Gardner, N.P., Lazar, M.A., and Flier, J.S. (2007). PPARγ regulates adipose triglyceride lipase in adipocytes *in vitro* and *in vivo*. Am. J. Physiol. Endocrinol. Metab. *293*, E1736–E1745. https://doi.org/10.1152/ajpendo.00122.2007.
27. Lin, F.T., and Lane, M.D. (1994). CCAAT/enhancer binding protein alpha is sufficient to initiate the 3T3-L1 adipocyte differentiation program. Proc. Natl. Acad. Sci. USA *91*, 8757–8761. https://doi.org/10.1073/pnas.91.19.8757.
28. Tang, Q.-Q., Otto, T.C., and Lane, M.D. (2003). CCAAT/enhancer-binding protein β is required for mitotic clonal expansion during adipogenesis. Proc. Natl. Acad. Sci. USA *100*, 850–855. https://doi.org/10.1073/pnas.0337434100.
29. Wang, N.D., Finegold, M.J., Bradley, A., Ou, C.N., Abdelsayed, S.V., Wilde, M.D., Taylor, L.R., Wilson, D.R., and Darlington, G.J. (1995). Impaired energy homeostasis in C/EBP alpha knockout mice. Science *269*, 1108–1112. https://doi.org/10.1126/science.7652557.
30. Rosen, E.D., Sarraf, P., Troy, A.E., Bradwin, G., Moore, K., Milstone, D.S., Spiegelman, B.M., and Mortensen, R.M. (1999). PPAR gamma is required for the differentiation of adipose tissue *in vivo* and *in vitro*. Mol. Cell *4*, 611–617. https://doi.org/10.1016/s1097-2765(00)80211-7.
31. Lee, J.-E., Schmidt, H., Lai, B., and Ge, K. (2019). Transcriptional and Epigenomic Regulation of Adipogenesis. Mol. Cell Biol. *39*, e00601-18. https://doi.org/10.1128/mcb.00601-18.
32. Farmer, S.R. (2006). Transcriptional control of adipocyte formation. Cell Metab. *4*, 263–273. https://doi.org/10.1016/j.cmet.2006.07.001.
33. Wu, X., and Zhang, Y. (2017). TET-mediated active DNA demethylation: mechanism, function and beyond. Nat. Rev. Genet. *18*, 517–534. https://doi.org/10.1038/nrg.2017.33.

34. Lisanti, S., von Zglinicki, T., and Mathers, J.C. (2012). Standardization and quality controls for the methylated DNA immunoprecipitation technique. Epigenetics *7*, 615–625. https://doi.org/10.4161/epi.20028.
35. Niehof, M., Kubicka, S., Zender, L., Manns, M.P., and Trautwein, C. (2001). Autoregulation enables different pathways to control CCAAT/enhancer binding protein B (C/EBPB) transcription *in vivo* and *in vitro*. J. Mol. Biol. *309*, 855–868. https://doi.org/10.1006/jmbi.2001.4708.
36. Yin, X., Hu, L., and Xu, Y. (2022). Structure and Function of TET Enzymes. Adv. Exp. Med. Biol. *1389*, 239–267. https://doi.org/10.1007/978-3-031-11454-0_10.
37. Hu, L., Li, Z., Cheng, J., Rao, Q., Gong, W., Liu, M., Shi, Y.G., Zhu, J., Wang, P., and Xu, Y. (2013). Crystal Structure of TET2-DNA Complex: Insight into TET-Mediated 5mC Oxidation. Cell *155*, 1545–1555. https://doi.org/10.1016/j.cell.2013.11.020.
38. Park, Y.-K., and Ge, K. (2017). Glucocorticoid Receptor Accelerates, but Is Dispensable for, Adipogenesis. Mol. Cell Biol. *37*, e00260-16. MCB.00260-00216. https://doi.org/10.1128/mcb.00260-16.
39. Krueger, K.C., Costa, M.J., Du, H., and Feldman, B.J. (2014). Characterization of Cre recombinase activity for *in vivo* targeting of adipocyte precursor cells. Stem Cell Rep. *3*, 1147–1158. https://doi.org/10.1016/j.stemcr.2014.10.009.
40. Berry, R., and Rodeheffer, M.S. (2013). Characterization of the adipocyte cellular lineage *in vivo*. Nat. Cell Biol. *15*, 302–308. https://doi.org/10.1038/ncb2696.
41. Yildirim, O., Li, R., Hung, J.H., Chen, P.B., Dong, X., Ee, L.S., Weng, Z., Rando, O.J., and Fazzio, T.G. (2011). Mbd3/NURD complex regulates expression of 5-hydroxymethylcytosine marked genes in embryonic stem cells. Cell *147*, 1498–1510. https://doi.org/10.1016/j.cell.2011.11.054.
42. Jones, P.L., Veenstra, G.J., Wade, P.A., Vermaak, D., Kass, S.U., Landsberger, N., Strouboulis, J., and Wolffe, A.P. (1998). Methylated DNA and MeCP2 recruit histone deacetylase to repress transcription. Nat. Genet. *19*, 187–191. https://doi.org/10.1038/561.
43. Nan, X., Ng, H.H., Johnson, C.A., Laherty, C.D., Turner, B.M., Eisenman, R.N., and Bird, A. (1998). Transcriptional repression by the methyl-CpG-binding protein MeCP2 involves a histone deacetylase complex. Nature *393*, 386–389. https://doi.org/10.1038/30764.
44. Ng, H.H., Zhang, Y., Hendrich, B., Johnson, C.A., Turner, B.M., Erdjument-Bromage, H., Tempst, P., Reinberg, D., and Bird, A. (1999). MBD2 is a transcriptional repressor belonging to the MeCP1 histone deacetylase complex. Nat. Genet. *23*, 58–61. https://doi.org/10.1038/12659.
45. Wade, P.A., Gegonne, A., Jones, P.L., Ballestar, E., Aubry, F., and Wolffe, A.P. (1999). Mi-2 complex couples DNA methylation to chromatin remodelling and histone deacetylation. Nat. Genet. *23*, 62–66. https://doi.org/10.1038/12664.
46. Kokura, K., Kaul, S.C., Wadhwa, R., Nomura, T., Khan, M.M., Shinagawa, T., Yasukawa, T., Colmenares, C., and Ishii, S. (2001). The Ski protein family is required for MeCP2-mediated transcriptional repression. J. Biol. Chem. *276*, 34115–34121. https://doi.org/10.1074/jbc.M105747200.
47. Rozenberg, J.M., Shlyakhtenko, A., Glass, K., Rishi, V., Myakishev, M.V., FitzGerald, P.C., and Vinson, C. (2008). All and only CpG containing sequences are enriched in promoters abundantly bound by RNA polymerase II in multiple tissues. BMC Genom. *9*, 67. https://doi.org/10.1186/1471-2164-9-67.
48. Deplus, R., Delatte, B., Schwinn, M.K., Defrance, M., Méndez, J., Murphy, N., Dawson, M.A., Volkmar, M., Putmans, P., Calonne, E., et al. (2013). TET2 and TET3 regulate GlcNAcylation and H3K4 methylation through OGT and SET1/COMPASS. Embo J *32*, 645–655. https://doi.org/10.1038/emboj.2012.357.
49. Fox, K.E., Fankell, D.M., Erickson, P.F., Majka, S.M., Crossno, J.T., Jr., and Klemm, D.J. (2006). Depletion of cAMP-response element-binding protein/ATF1 inhibits adipogenic conversion of 3T3-L1 cells ectopically expressing CCAAT/enhancer-binding protein (C/EBP) alpha, C/EBP beta, or PPAR gamma 2. J. Biol. Chem. *281*, 40341–40353. https://doi.org/10.1074/jbc.M605077200.
50. Rivers, L.E., Young, K.M., Rizzi, M., Jamen, F., Psachoulia, K., Wade, A., Kessaris, N., and Richardson, W.D. (2008). PDGFRA/NG2 glia generate myelinating oligodendrocytes and piriform projection neurons in adult mice. Nat. Neurosci. *11*, 1392–1401. https://doi.org/10.1038/nn.2220.
51. Zhao, X., Dai, J., Ma, Y., Mi, Y., Cui, D., Ju, G., Macklin, W.B., and Jin, W. (2014). Dynamics of ten-eleven translocation hydroxylase family proteins and 5-hydroxymethylcytosine in oligodendrocyte differentiation. Glia *62*, 914–926. https://doi.org/10.1002/glia.22649.
52. Xu, Y., Wu, F., Tan, L., Kong, L., Xiong, L., Deng, J., Barbera, A.J., Zheng, L., Zhang, H., Huang, S., et al. (2011). Genome-wide Regulation of 5hmC, 5mC, and Gene Expression by Tet1 Hydroxylase in Mouse Embryonic Stem Cells. Mol. Cell *42*, 451–464. https://doi.org/10.1016/j.molcel.2011.04.005.
53. Adelmant, G., Garg, B.K., Tavares, M., Card, J.D., and Marto, J.A. (2019). Tandem Affinity Purification and Mass Spectrometry (TAP-MS) for the Analysis of Protein Complexes. Curr. Protoc. Protein Sci. *96*, e84. https://doi.org/10.1002/cpps.84.

STAR★METHODS

KEY RESOURCES TABLE

REAGENT or RESOURCE	SOURCE	IDENTIFIER
Antibodies		
Rabbit polyclonal anti-TET1	Abcam	Cat#ab157004; RRID: AB_3073779
Rabbit polyclonal anti-TET2	Abcam	Cat#ab124297; RRID: AB_2722695
Rabbit polyclonal anti-TET3	Abcam	Cat#Ab139805; RRID: AB_3073778
Rabbit polyclonal anti-CREB	proteintech	Cat#12208-1-AP; RRID: AB_2245417
Mouse monoclonal anti-CREB	Santa Cruz	Cat#sc-374227; RRID: AB_10989935
Rabbit monoclonal anti-phospho-CREB (Ser133)	CST	Cat#9198; RRID: AB_2561044
Rabbit polyclonal anti-C/EBPβ	Santa Cruz	Cat#SC-150; RRID: AB_2260363
Rabbit polyclonal anti-C/EBPα	Santa Cruz	Cat#SC-61; RRID: AB_631233
Mouse monoclonal anti- C/EBPβ	Abcam	Cat#Ab15050; RRID: AB_301598
Rabbit polyclonal anti-PPARγ	Proteintech	Cat#16643-1-AP; RRID: AB_10596794
Rabbit polyclonal anti-FABP4	Proteintech	Cat#12802-1-AP; RRID: AB_2102442
Rabbit polyclonal anti-5hmC	Active motif	Cat#39791; RRID: AB_2630381
Mouse monoclonal anti-5mC	Active motif	Cat#39649; RRID: AB_2687950
Rabbit polyclonal anti-Flag	Sigma-Aldrich	Cat#F7425; RRID: AB_439687
Rabbit polyclonal anti-HA	CST	Cat#3724; RRID: AB_1549585
Goat polyclonal anti-LaminB	Santa Cruz	Cat#SC-6216; RRID: AB_648156
Bacterial and virus strains		
LentiCRISPRv2-CREB-1 plasmid	This paper	N/A
LentiCRISPRv2-CREB-2 plasmid	This paper	N/A
LentiCRISPRv2-TET2-1 plasmid	This paper	N/A
LentiCRISPRv2-TET2-2 plasmid	This paper	N/A
pLV-CS2.0-FLAG-HA-TET2	This paper	N/A
Chemicals, peptides, and recombinant proteins		
Type II collagenase	Sigma	Cat#C6885
polyethylenimine	Polysciences	Cat#23966-1
Polybrene	Sigma	Cat#H9268
TurboFect transfection reagent	Thermo	Cat#R0531
TRIzol	Invitrogen	Cat#15596026
IP lysis buffer	Beyotime	Cat#P0013
UltraSYBR Mixture	CWBIO	Cat#0957
Dexamethasone	Sigma-Aldrich	Cat#D1756
IBMX	Sigma-Aldrich	Cat#I5879
Rosiglitazone	MCE	Cat#HY-17386
Insulin (human)	MCE	Cat#HY-P0035
Nile Red	Sigma	Cat# 72485
DAPI	Beyotime	Cat#C1002
Oil Red O	Sangon	Cat# A600395
Methylene blue trihydratee	Yuanye	Cat#S19043
Critical commercial assays		
Cell-counting-kit-8 (CCK8) assay kit	APExBIO	Cat#K1018
BCA assay kit	Thermo Scientific	Cat#23227

(*Continued on next page*)

Continued

REAGENT or RESOURCE	SOURCE	IDENTIFIER
hematoxylin-eosin kit	Boster	Cat#AR1180
ChIP Assay Kit	Beyotime	Cat#P2078
5× All in One kit	Abm	Cat#G490
Nonesterified free acids assay kit	Nanjing Jiancheng	Cat#A042-2-1
Alanine aminotransferase assay kit	Nanjing Jiancheng	Cat#C009-2-1
Aspartate aminotransferase assay kit	Nanjing Jiancheng	Cat#C010-2-1
Total cholesterol assay kit	Nanjing Jiancheng	Cat#A111-1-1
Triglyceride assay kit	Nanjing Jiancheng	Cat#A110-1-1
Resistin Assay Kit	Nanjing Jiancheng	Cat#H175
Adiponectin Assay Kit	Nanjing Jiancheng	Cat#H179
Experimental models: Cell lines		
Mouse: 3T3-L1 cell	Laboratory of Qi-qun Tang; Qi-Qun Tang and M. Daniel Lane. 1999[18]	N/A
HEK 293T cell	ATCC	Cat# CRL-3216
Experimental models: Organisms/strains		
Tet2$^{flox/flox}$ mice	Jackson Laboratory	strain #: 017573
PdgfRα-Cre mice	Jackson Laboratory	strain #: 013148
PdgfRα-Cre;Tet2$^{flox/flox}$ mice.	This paper	N/A
Oligonucleotides		
Primers for genotyping, see Table S2	This paper	N/A
Primers for RT-qPCR, see Table S3	This paper	N/A
gRNA sequences for CRISPR/Cas9, see Table S4	This paper	N/A
Primers for ChIP and hMeDIP RT-qPCR, see Table S5	This paper	N/A
Recombinant DNA		
pLV-FLAG-TET2	This paper	N/A
pLV-FLAG-TET2 (1-491)	This paper	N/A
pLV-FLAG-TET2 (1-1041)	This paper	N/A
pLV-FLAG-TET2 (492-1041)	This paper	N/A
pLV-FLAG-TET2 (1042-1921)	This paper	N/A
pLV-FLAG-TET2 (1042-1237)	This paper	N/A
pLV-FLAG-TET2 (1238-1921)	This paper	N/A
pLV-HA-CREB	This paper	N/A
pLV-HA-C/EBPβ	This paper	N/A
FH-Tet2-pEF	Addgene	Cat#41710; RRID: Addgene_41710
λDNA	Thermo Scientific	Cat#SD0021
Software and algorithms		
ImageJ_v1.8.0	ImageJ, NIH	https://imagej.net/ij/download.html
GraphPad Prism 8.3.0	GraphPad Software, LLC	https://www.graphpad.com/
Integrative genomics viewer	Broad Institute and the Regents of the University of California	https://igv.org/app
Peaks Studio X software	Bioinformatics Solutions Inc.	https://www.bioinfor.com/
Other		
High-fat diet	Research Diets	Cat#D12492i
Centrifugal filter units (100 KDa)	Millipore	Cat#UFC910096
Anti-Flag Magnetic Beads	MCE	Cat#HY-K0207;
Protein A/G magnetic beads	MCE	Cat#HY-K0202

RESOURCE AVAILABILITY

Lead contact

Further information should be directed to and will be fulfilled by the lead contact, Boan Li (bali@xmu.edu.cn).

Materials availability

All plasmids and mouse line generated in this study are available from the lead contact with a completed materials transfer agreement.

Data and code availability

All data reported in this paper will be shared by the lead contact upon request.
This paper does not report original code.
Any additional information required to reanalyze the data reported in this paper is available from the lead contact upon request.

EXPERIMENTAL MODEL AND STUDY PARTICIPANTS DETAILS

Cell lines

3T3-L1 preadipocytes were kindly donated by Qi-Qun Tang, Fudan University Shanghai Medical College. HEK 293T cells were purchased from the American Type Culture Collection (ATCC). Primary SVF cells were isolated from iWAT. The 3T3-L1 preadipocytes were cultured in high-glucose DMEM with 10% FBS at 8% CO_2 and 37°C. HEK 293T cells were cultured in high-glucose DMEM with 10% FBS at 5% CO_2, 37°C. SVFs from WAT were maintained in high-glucose DMEM, 1% penicillin/streptomycin and 20% FBS at 8% CO_2, 37°C. The cell lines were authenticated by Short Tandem Repeat analysis. The cell lines were tested for mycoplasma contamination routinely.

For differentiation, confluent 3T3-L1 cells or SVF cells were cultured for an additional two days and induced to differentiate by treatment with a cocktail of methylisobutylxanthine (0.5 mM), dexamethasone (1 mM) and insulin (10 μg/mL) for 2 days. After 2 days, the cocktail was removed and replaced with insulin (10 μg/mL), and the cells were incubated for another 2 days. Then, the cells were cultured in general growth medium until harvest.

Mice

Tet2$^{flox/flox}$ mice and *PdgfRα-Cre* mice were purchased from Jackson Laboratory and kept under specific pathogen-free conditions at 22°C with a 12 hours light-dark cycle and free access to food and water. 3-month-old *Tet2*$^{flox/flox}$ mice were mated with *PdgfRα-Cre* mice, and the offspring (first generation) were genotyped to select *PdgfRα-Cre;Tet2*$^{flox/+}$ mice, which were then (8-10 weeks) backcrossed with *Tet2*$^{flox/flox}$ mice to generate *PdgfRα-Cre;Tet2*$^{flox/flox}$ mice. Male mice were used for all experiments. The animal studies were approved by the Institutional Animal Care and Use Committee of Xiamen University. All animal care was conducted in accordance with institutional guidelines.

The primers used for genotyping are shown in Table S2.

METHOD DETAILS

Isolation of adipose SVF and mature adipocytes

Inguinal adipose depots of 6-week-old C57BL/6 mice were minced and digested with digestion solution (3 mg/mL type II collagenase, 3% BSA in HBSS) for 1 hour at 37°C. The mixture was gently pipetted several times and centrifuged at 2300 rpm for 7 min at 4°C. The suspended adipocytes and the precipitated SVF were collected and lysed by TRIzol for subsequent RNA extraction and qPCR analysis.

Quantitative reverse transcription PCR

Total RNA was extracted from cells or tissues with TRIzol. First-strand cDNA was synthesized using a 5× All in One kit. An UltraSYBR Mixture and a PCR machine were used for the qPCR experiments. All experiments were performed in triplicate. The primers used in RT−qPCR are shown in Table S3.

Western blot analysis

Cells or tissues were lysed in 2% SDS lysis buffer (2% SDS, 50 mM Tris-HCl, pH 6.8) with the proteinase inhibitor cOmplete and PMSF. The lysates were sonicated briefly and boiled at 100°C for 10 min. The protein concentrations of the samples were quantified with a BCA assay kit. The samples were separated by SDS−PAGE and transferred to PVDF membranes. The membranes were sequentially incubated with blocking buffer (5% skim milk in TBST) for 60 min at room temperature, incubated with primary antibodies overnight at 4°C, incubated with secondary antibodies for 1 hour at room temperature and subjected to chemiluminescence imaging. All experiments were repeated three or more times.

Cell-counting-kit-8 (CCK-8) assay

Tet2-knockout and control 3T3-L1 preadipocytes (1×10^4) were placed into 96-well dishes for 4 days. Ten microliters of CCK-8 reagent were added to each well and incubated for 2 hours at 37°C, followed by absorbance readings at 450 nm at indicated time points.

Nile red staining

Stock solutions of Nile Red (50 μg/mL, 250×) and DAPI (5 mg/mL, 1000×) were prepared and stored protected from light. The cells were washed with PBS twice and fixed with 4% formaldehyde solution for 20 min. The fixed cells were stained with working solution (3% BSA, 0.2 μg/mL Nile Red, 5 μg/mL DAPI) for 10 min at room temperature away from light. The cells were washed with PBS to remove the extra solution and then photographed. All experiments were performed in triplicate.

Plasmids, lentivirus production and lentivirus-mediated gene transfer

For construction of CRISPR/Cas9 lentivirus plasmids, the gRNA sequences targeting *Tet2* and *Creb1*, which were designed at http://crispr.mit.edu/, were cloned into a lentiCRISPRv2 vector. The gRNA sequences are shown in Table S4. For construction of the C/EBPβ expression plasmid, the CDS of the canonical isoform LAP was cloned into a pLV-CS2.0-HA-puro lentivirus vector. For construction of the TET2 expression plasmid, the sequence of FLAG-HA-TET2 was amplified from FH-Tet2-pEF which was a gift from Anjana Rao and cloned into a pLV-CS2.0-bsd lentivirus vector. For generating truncation mutations, fragments of pLV-CS2.0-FH-TET2 were PCR amplified and spliced by ligation-independent cloning. For construction of the CREB expression plasmid, *Creb1* cDNA was PCR amplified and cloned into the pLV-CS2.0-HA-puro vector.

Lentiviruses were generated by co-transfecting target plasmids with the helper plasmids pVSV-G and pHR into HEK293T cells using TurboFect transfection reagent. For lentivirus-mediated gene transfer in 3T3-L1 preadipocytes, the lentiviruses were collected 48 hours after transfection and concentrated with centrifugal filter units. The cells were treated with Polybrene 1 hour before infection at 20%-30% confluence.

hMeDIP

The protocols used for hMeDIP have been described in a previous study.[52] Genomic DNA was purified from 3T3-L1 cells and primary SVF cells, and dissolved in TE buffer (pH 8.0). Two micrograms of genomic DNA from each sample were sonicated. A fragment amplified from λDNA was purified by agarose gel electrophoresis and gel extraction. The primers used to generate the fragment from λDNA were 5′-GTGAGGTGAATGTGGTGAAGT-3′ (forward primer) and 5′- TCGCAGAGATAAAACACGCT-3′ (reverse primer). A total of 0.75 micrograms of sonicated genomic DNA and 5 nanograms of fragment amplified from λDNA were diluted in 300 μL of TE buffer for each sample. One microgram of IgG or antibody specific to 5hmC was added to each sample. Seventy microliters of protein A/G magnetic beads pre-blocked with 3% BSA in 1× IP buffer were added to pull down antibody–DNA complexes. Enrichment of the target regions was determined by qPCR using SYBR Green reagent. The primers used in hMeDIP-qPCR are shown in Table S5.

ChIP

ChIP was performed using a ChIP Assay Kit. 3T3-L1 cells were trypsinized to a single-cell suspension and then cross-linked with 1% formaldehyde at 37°C for 10 min. Chromatin samples were immunoprecipitated with 10 μg of IgG or antibody specific to TET2 or CREB and protein A/G magnetic beads pre-blocked with 3% BSA. Enrichment of the target regions was determined by qPCR using SYBR Green reagent. The primers used in ChIP-qPCR were the same as those used in hMeDIP.

Co-IP

For endogenous co-IP experiments, cells were washed with PBS three times and lysed in IP lysis buffer with the proteinase inhibitor cOmplete and PMSF for 15 min at 4°C. The lysates were sonicated briefly and centrifuged at 13000 rpm and 4°C for 10 min. The supernatants were precleared by incubating with pre-blocked magnetic protein A/G beads for 1 h at 4°C. The antibody against phospho-CREB or homologous IgG was added to the precleared samples, and the samples were incubated overnight at 4°C. The pre-blocked magnetic beads were added, and the samples were incubated for an additional 1 hour at 4°C. Then, the beads were washed with IP buffer three times and subjected to SDS–PAGE for analysis with appropriate antibodies. For exogenous co-IP, FH-TET2-pEF purchased from Addgene and/or an HA-C/EBPβ construct was transfected into HEK293T cells. Cells were collected at 24 hours after transfection, and co-IP was performed as described for endogenous co-IP. Antibodies against TET2 and C/EBPβ were used in co-IP. For determining TET2-CREB interaction, expression vectors for HA-CREB and different truncation mutants of FLAG-TET2 were transiently transfected into HEK293T cells. Cells lysates were subjected to co-IP with 10 μL pre-blocked anti-FLAG magnetic beads.

IP-mass spectrometry

To identify proteins bound to TET2, 3T3-L1 cells stably expressing FLAG-HA-TET2 were harvested from ten 150 mm dishes at 4 hours after induction. Subcellular fractionation and lysis of cell nucleus were as described.[53] Cells were washed with DPBS twice and centrifuged for 3 min at 300 × g, 4°C. Cell pellets were resuspended with 5 times the cell pellet volume (CPV) of hypotonic buffer (10 mM Tris-Cl (pH 7.3), 10 mM KCl, 1.5 mM $MgCl_2$, 0.007% (v/v) 2-mercaptoethanol and protease inhibitor cocktail) and then centrifuged for 3 min at 800 × g, 4°C. Cell pellets were resuspended with one CPV of hypotonic buffer and incubated for 10 min on ice, then sheared with Dounce homogenizer to release nuclei. The content of homogenizer was centrifuged for 10 min at 1000 × g, 4°C. The nuclear pellets were washed with hypotonic buffer and then subjected to immunoprecipitation (IP) experiments. The binding proteins were denatured using SDS and separated by SDS-PAGE gel electrophoresis. After staining of gel with Coomassie blue, the lanes were excised into 1 mm × 1 mm dice. The segments between

40-50 kD were collected as one sample (YJ-2), while the others were collected as another sample (YJ-3). Excised gel segments were subjected to in-gel trypsin digestion and dried. Samples were analyzed on a nanoElute (Bruker) coupled to a timsTOF Pro (Bruker) equipped with a CaptiveSpray source. Peptides were dissolved in 10 μL 0.1% formic acid and were auto-sampled directly onto a homemade C18 column (35 cm × 75 μm i.d., 1.9 μm 100 Å). Samples were then eluted for 60 min with linear gradients of 3–35% acetonitrile in 0.1% formic acid at a flow rate of 300 nL/min. Mass spectrometry data were acquired with a timsTOF Pro mass spectrometer (Bruker) operated in PASEF mode. The raw files were analyzed by Peaks Studio X software against Uniprot database. The data from both samples were merged during the analysis.

Body weight, body composition

Body weight of 3-week-old mice was monitored weekly for 17 weeks. Body composition of 20-week-old mice was measured with an EchoMRI-100H.

Food and water intake and movement measurements

6-week-old mice were housed individually in metabolic cages of a small animal metabolism measurement and analysis system with free access to food and water. Food and water intake and movement were monitored every 30 min for each mouse over a period of 5 days.

Hematoxylin and eosin (H&E) staining

Pieces of iWAT, eWAT and liver from 20-week-old mice fed an HFD were fixed with 4% paraformaldehyde in PBS for 24 hours at room temperature and then subjected sequentially to dehydration in a 50%, 75%, 85%, 95% and 100% alcohol gradient for 5 hours. Then, they were cleared in xylene, paraffin-embedded, and sectioned at a thickness of 5 μm. The sections were deparaffinized, rehydrated, and stained with an H&E kit.

Blood analysis

Blood was sampled from 20-week-old mice's eyes and natural coagulation in ambient temperature for 2 hours, then centrifugate at 2000 rpm for 20 min. The supernatant serum was collected carefully and tested for total cholesterol, free fatty acid, triglyceride, AST, ALT, adiponectin and resistin following the instruction.

Glucose tolerance test (GTT)

20-week-old mice were fasted for 16 hours prior to the test. At baseline, the blood glucose levels were measured. Glucose was intraperitoneally injected at Time 0 (1 g/kg). The blood glucose levels were measured and recorded at 15 min, 30 min and 60 min.

Insulin tolerance test (ITT)

20-week-old mice were fasted for 6 hours prior to the test. At baseline, the blood glucose levels were measured. Insulin was intraperitoneally injected at Time 0 (0.5 U/kg). The blood glucose levels were measured and recorded at 15 min, 30 min and 60 min.

QUANTIFICATION AND STATISTICAL ANALYSIS

Each experiment was repeated at least three times. The results of representative experiments are shown unless stated otherwise. Statistical comparisons were performed by unpaired two-tailed Student's t test. A normal distribution was assumed. All statistical tests were performed with GraphPad Prism 8 software. The differences were considered statistically significant at $p < 0.05$ and reported as follows (*$p < 0.05$, **$p < 0.01$, ***$p < 0.001$; ****$p < 0.0001$; ns, no significance). Investigators were not blinded to group allocation during experiments.